National University of Science and Technology
POLITEHNICA Bucharest
Faculty of Energy
Department of Hydraulics, Hydraulic Machines
and Environmental Engineering

Ph. D THESIS

-SUMMARY-

PROPORTIONAL ELECTRO PNEUMATIC SERVOMECHANISM, SEPP, USED FOR THE ACTUATION OF VALVES IN THE ENERGY INDUSTRY

Author: PhD. STUDENT Eng. Valentin-Nicolae COCOCI

Supervisor: prof. dr. ing. Carmen-Anca SAFTA

Bucharest, 2023

Abstract

The thesis ''Proportional electro pneumatic servomechanism, SEPP, used for the actuation of valves in the energy industry'', is a research paper that, through numerical simulations and experimental tests, finds the dynamic performance of an electropneumatic linear positioning servomechanism used in controling of valves applied in various applications in the energy industry.

The originality of the thesis is given by the use of proportional distributors as a control element of the linear pneumatic actuator. Pneumatic proportional distributors are equipment developed over the past 35 years that have begun to successfully replace the much more expensive pneumatic servo valves than proportional distributors.

The main objectives of the thesis are:

1. In-depth bibliographic study to determine the development of the studied subject, from a theoretical and experimental point of view;
2. Theoretical study regarding the mathematical modeling of the pneumatic actuation system with proportional distributor;
3. Realization of a pneumatic actuation scheme of electropneumatic servomechanism type for linear positioning with proportional distributor;
4. Determination of the dynamic performances of the SEPP through numerical simulations;
5. Experimental determination of dynamic performance of SEPP, numerical model calibration and regulator connection.

Chapter 1 presents a brief introduction to the topic of the paper. The objectives and motivation of this paper are presented. Also here is a brief presentation of the thesis content.

In **Chapter 2**, a brief history about the development of the pneumatic drives fields and are highlighted the market trends in the field of pneumatic systems. Also it is presented the current, theoretical and experimental status for various applications of the pneumatic actuation and servoactuation systems mentioned in the specialized literature.

Chapter 3 is dedicated to the description of pneumatic servomechanisms, describing eachc omponent of these systems. Also, in this chapter, the properties of air (the working fluid in pneumatic drives), pressure domains, flow rates and flow diameters, examples of closed and open lump pneumatic drive schemes, but also experimental research carried out by other authors are mentioned , in the subject of this chapter.

The theoretical study of compressible fluid flow through orifices and nozzles, the flow-pressure characteristic through the orifices of the pneumatic distributor, and the equations that define the mathematical model of an electropneumatic linear positioning servomechanism, are presented in **Chapter 4**.

The results of the numerical simulations that are the basis for the performance validation of the pneumatic system operated by a proportional distributor are described in the **Chapter 5**. In this chapter, the types of software that can be used for the numerical simulation, the working methodology used for the numerical simulation, and the numerical results simulations for closed and open loop pneumatic drives are presented. Also, the results of the numerical simulations in the case of the electropneumatic positioning servomechanism used in the control

of the supply valve of the aerators are mentioned the biological stage of a sewage treatment plant are presented.

The experimental validation of the results obtained through the numerical simulations is presented in **Chapter 6**. The work methodology, the results of the experimental tests, the comparison of the numerical results with the experimental ones, and finally conclusions are presented.

Chapter 7 presents the synthesis of the main scientific and technical contributions according to the three directions of thesis development: theoretical research, numerical simulations, experimental tests.

At the end of the thesis you will find the bibliography and appendices.

The results of the numerical simulations were obtained with the help of the AMESim software from SIEMENS, and the experimental research was carried out, for the most part, with the help of Festo Didactic Romania equipment. The experimental tests were carried out both in the Honeywell Laboratory of the Faculty of Automation and Computers of the Polytechnic University of Bucharest, and in the Automation Laboratory of Festo Didactic Romania.

Keywords: pneumatic actuator, pneumatic proportional distributor, compressible fluid, energy industry, mathematical modeling, numerical simulations, experimental tests, valve.

Special thanks

The writing and publication of this paper was possible thanks to the support of several people who supported and encouraged me. I would like to express my deep gratitude to:

Professor Carmen-Anca SAFTA, the scientific supervisor, for the constant support from a scientific, technical and moral point of view during the entire period of preparation and development of the thesis. I thank her for his openness and patience.

Prof. Dr. Eng Nicolae VASILIU for the constructive advice and encouragement he gave me during the conversations we had**.**

To the members of the thesis guidance committee:

- **Mr. Conf. dr. ing Constantin CALINOIU**, for his constant availability and the time given to carry out the experimental tests in the Honeywell laboratory of the Faculty of Automation and Computers from the Polytechnic University of Bucharest and my training in the use of software for the realization of numerical simulations.
- **Mr. prof. dr. ing Ciprian LUPU**, for the constant availability and the time given in the various problems encountered in carrying out the experimental tests, but also for the fact that he made available to us the Honeywell laboratory within the Faculty of Automation and Computers of the Polytechnic University of Buchares.
- **Mr. prof. dr. ing. Alexandru MARIN** for the useful suggestions and observations given during the realization of the work.
- **Mr. prof. dr. matem. Andrei HALANAY** for the support given in the realization of the mathematical model.
- **Mr. conf. dr. ing. Andrei DRUMEA** for the beneficial comments provided throughout the development of the paper.

The long-term support offered by the Festo Didactic Romania team, which was essential in completing the test stand developed by the author. The technical competence of Mr. Adelin PLACINTARU was crucial for the creation of the experimental test stand. I also thank you Festo team for providing me with all the necessary technical documentation.

I would like to thank the members of the thesis examination committee for the suggestions and observations useful for the completion of the work:

1. Prof.dr.ing. Radu Florin PORUMB
2. Prof.dr.ing. Carmen-Anca SAFTA
3. Prof.dr.ing. Nicolae VASILIU
4. CSI dr.ing. Vergil MURARU
5. Prof.dr.ing. Ilare BORDEAȘU

Last but not least, I thank my wife and parents for their support and unconditional moral support during my doctoral studies.

Summary

Chapter I 7
INTRODUCTION 7
1.1. Overview 7
1.2. Goals and motivation 8
1.3. Analysis of the bibliographic study 9
1.4. Thesis structure 10
Chapter II 11
2.1 Overview 11
2.1.1 Brief history of the development of the field of pneumatic drives 11
2.1.2 Market trends of pneumatic actuation systems 11
2.2. Structures of electropneumatic servomechanisms 12
2.3. Theoretical research on electropneumatic components 12
2.4 Experimental research on electropneumatic components 14
2.5. Technological innovations in pneumatic drive applications 15
Chapter III 16
3.1 Overview 16
3.2. Air properties 17
3.3. Pressure and flow domains 18
3.4. Pneumatic equipment 19
3.5. Electropneumatic drives 20
Chapter IV 21
MATHEMATICAL MODELING OF PNEUMATIC SERVOMECHANISMS WITH LINEAR ACTUATORS 21
4.1. Overview 21
4.2. Air flow through nozzles and holes 21
4.3. Mass flow characteristic through variable area orifices 24
4.4. Numerical simulations on the dynamic behavior of proportional distributors 26
4.5. Nonlinearities in the operation of electropneumatic servomechanisms 28
4.6. Control methods in pneumatic positioning systems 30
4.7. The mathematical model associated with the electropneumatic servomechanism 31
Chapter V 34
NUMERICAL SIMULATIONS TO DETERMINE THE PERFORMANCE OF THE ELECTROPNEUMATIC SERVO-MECHANISM WITH PROPORTIONAL DISTRIBUTOR 34
5.1 Overview 34
5.3. Work methodology in Simcenter Amesim 34
5.4. Numerical simulation of the dynamic behavior of linear pneumatic actuators 35
5.5. Dynamic behavior of electropneumatic positioning servomechanisms with symmetric and asymmetric actuators 41

5.6. Dynamic behavior of an electropneumatic servomechanism for actuation of a butterfly valve ... 45

Chapter VI ... 47

EXPERIMENTAL DETERMINATION OF ELECTROPNEUMATIC SERVO-MECHANISM PERFORMANCE ... 47

6.1. Overview ... 47

6.2. Structure of the test stand ... 47

6.3. Work methodology ... 47

6.4. Experimental results ... 49

6.5. Conclusions and comparison with numerical results ... 54

Chapter VII ... 56

SYNTHESIS OF THE MAIN SCIENTIFIC AND TECHNICAL CONTRIBUTIONS OF THE WORK. FUTURE DIRECTIONS OF RESEARCH ... 56

7.1. General conclusions ... 56

7.2. Original contributions ... 57

7.3. Future research directions ... 58

Thesis bibliography ... 59

Chapter I

INTRODUCTION

1.1. Overview

The beginning of the 21st century is technologically defined by the digitization process, culminating in the development of the concept of Industry 4.0 (4IR-th 4th Industrial Revolution). Digitization allows the conversion of analog data into digital format, which facilitates the transmission of information in real time [101].

The digitization process has led to the much wider use of pneumatic actuators, due to the advantages brought by the transmission of information in real time, through the new structures of miniaturized and embedded electronic systems in many of the pneumatic actuator components. This transmission of data in real time determined the correction of a significant problem in the field of pneumatic drives, namely the correction of non-linearities due to the compressibility of the gas, the flow of air through the holes, the frictional forces developed during the movement of the mechanical elements, the hysteresis due to the magnetic and electrical materials in the composition pneumatic command and control elements.

Pneumatic systems convert the energy of compressed air into mechanical energy, which can be used as mechanical work transmitted to execution elements such as pneumatic actuators (linear or rotary) [1].

In the field of robots, depending on the mobility, respectively the number of degrees of freedom, several linear or angular positioning systems can be used. This is also the case with the Kokoro humanoid robot, Figure 1.2, which has 38 degrees of freedom, 114 sensors and 76 control loops. The robot uses FESTO MPYE type proportional distributors [103].

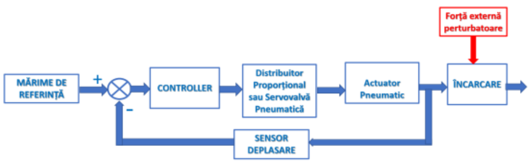

Figure 1.1. Block diagram of an electropneumatic linear positioning system

Figure 1.2. The humanoid robot "Kokoro" FESTO MPYE type proportional distributors for electropneumatic servo-actuators, [103]

Modern electropneumatic positioning systems use proportional distributors in their structure to control the air flow required by the actuator. Like the electropneumatic servovalves, the proportional distributors are electropneumatic amplifiers that at a given current command (voltage or intensity) the delivered flow rate is proportional to the command. The performance of proportional valves is not equal to the performance of pneumatic servo valves, but the manufacturing and purchase costs are much lower. Given that from a technical point of view the performances of proportional distributors ([135] hysteresis 3%; repeatability 3%; sensitivity 0.05%; linearity 3%; response time < 50 ms) are close to the performances of servo valves, the use of proportional distributors in systems positioning is common, and technical interest in the study of these systems has increased.

1.2. Goals and motivation

The thesis Proportional electropneumatic servomechanism, SEPP, for the actuation of valves in the energy industry, is a research paper that, through numerical simulations and experimental tests, determines the dynamic performance of an electropneumatic linear positioning servomechanism used in the controling of various applications in the energy industry .

The novelty of the thesis is given by the use of proportional distributors as a control element of the linear pneumatic actuator. Pneumatic proportional distributors are equipment developed over the past 35 years that have begun to successfully replace the much more expensive pneumatic servo valves than proportional distributors.

The proposed pneumatic actuation system is a positioning servomechanism, composed of a pneumatic cylinder (actuator) driven by a proportional distributor operating in a closed loop.

Figure 1.3 shows the experimental stand for the experimental identification of the components of the electropneumatic servomechanism.

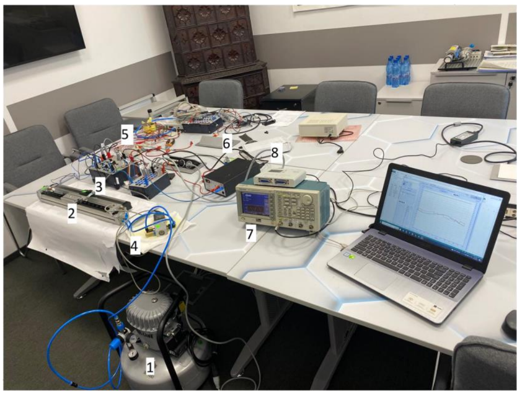

Figure 1.3. Experimental stand: 1- air compressor; 2- pneumatic cylinder; 3- linear potentiometer; 4- proportional distributor 5/3; 5- PID; 6-source 24 V; 7- signal generator; 8- data acquisition board [17]

The behavior numerical modeling of the studied electropneumatic servomechanism was carried out using the Simcenter Amesim numerical simulation platform. Figure 1.4 shows the used numerical simulation scheme. In the thesis, the experimental results are compared with the numerical ones.

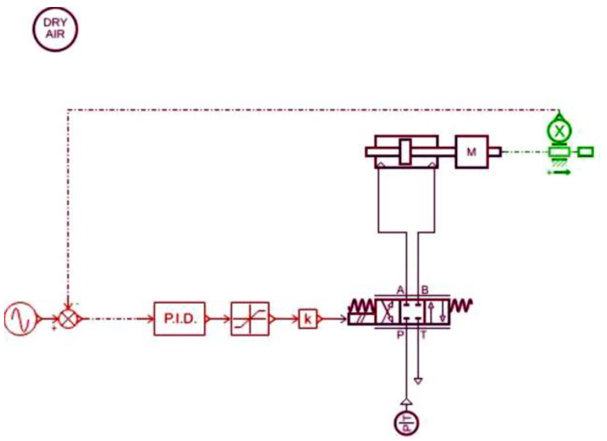

Figure 1.4. Numerical simulation scheme [17]

In Fig. 1.5 shows an example of the use of proportional distributors in the pressurized air supply systems of the aerators in the bioreactors of a sewage treatment plant. If the fluid flow is high and the installation requires flow control through butterfly valves, then their actuation can be done with a pneumatic positioning servo, as proposed in the present work.

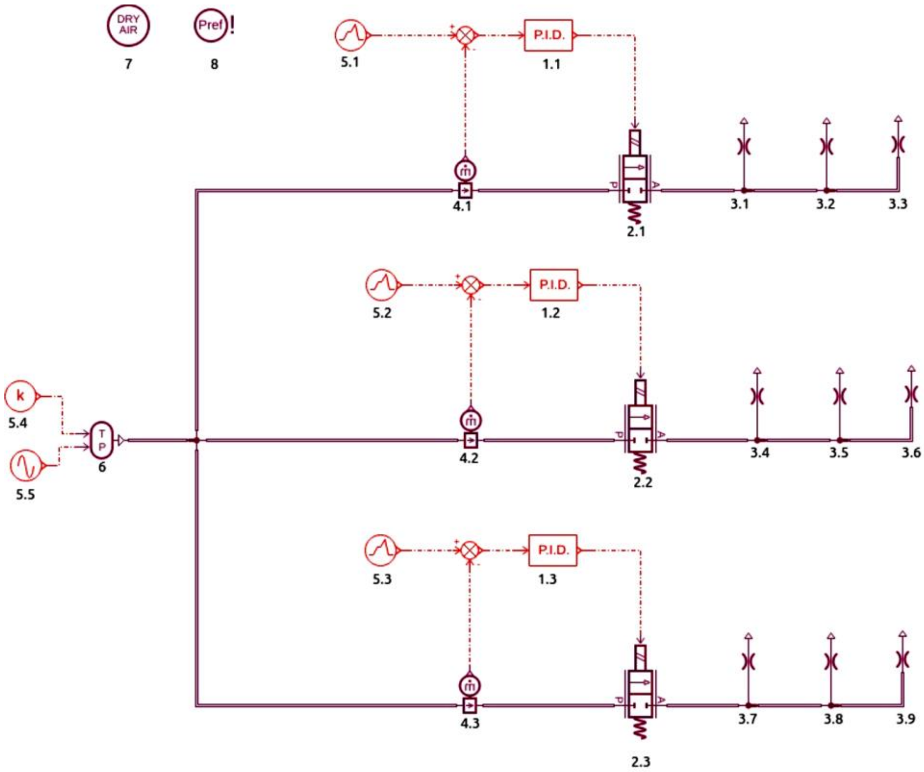

Figure 1.5. Drive scheme with proportional pneumatic distributors, proposed for the control of aerators in a water treatment plant [48]

The main objectives of the thesis are:

1. A depth bibliographic study to determine the development of the studied subject, from a theoretical and experimental point of view;
2. Theoretical study regarding the mathematical modeling of the pneumatic actuation system with proportional distributor;
3. Realization of a pneumatic actuation scheme of electrohydraulic servomechanism type for linear positioning with proportional distributor;
4. Determination by numerical simulations of the dynamic performances of the SEPP;
5. Experimental determination of dynamic performance of SEPP, numerical model calibration and regulator connection

1.3. Analysis of the bibliographic study

More than 260 bibliographic references were studied for the realization of the thesis, of which approximately 148 were actually used and cited in the thesis.

Figures 1.6 – 1.9 present a classification of the thesis bibliography, according to the type of references, the year of publication, the language used in writing the references and the number of references corresponding to each chapter.

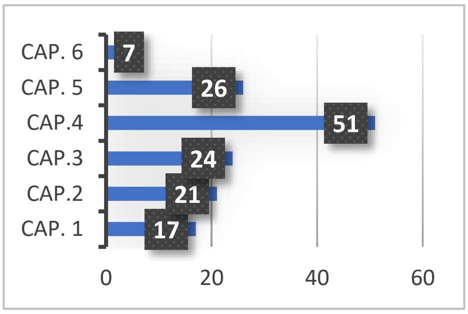

Figure 1.6. Bibliographic titles by chapters

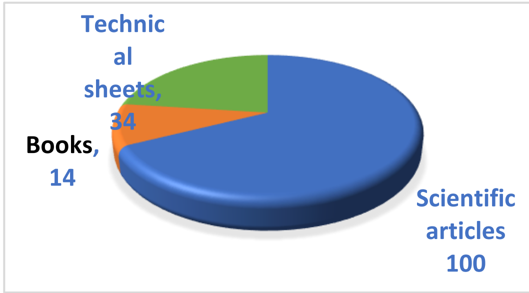

Figure 1.7. The structure of the bibliography according to the type of bibliographic references

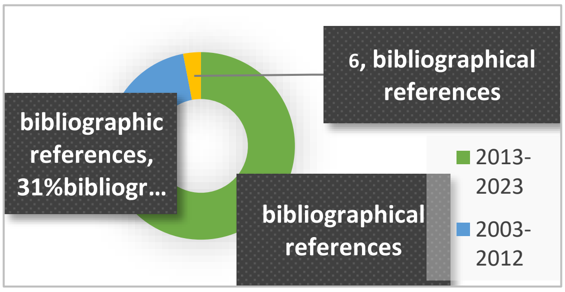

Figura 1.8. The structure of the bibliography according to the year of publication of the bibliographic references

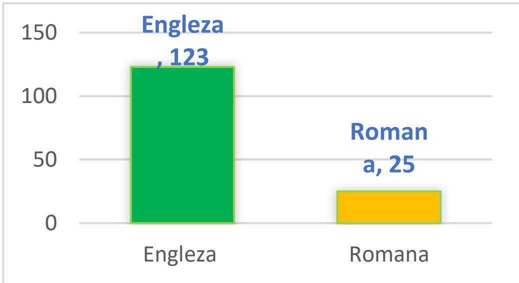

Figura 1.9. Bibliography structure according to the language used for publishing bibliographic references

After the analysis done, in figures 1.6 - 1.9 it can be seen that a number of 100 scientific articles, 14 books and 34 technical sheets were studied and used for the conception of the thesis. The available bibliography is current as 66% of the bibliographic references were published between 2013-2023 and only 3% before 2002.

A majority of 83% of the bibliographic references used are written in English, the remaining 17% being written in Romanian.

1.4. Thesis structure

The thesis is structured in 7 chapters, ordered according to the main objectives and the aim pursued by the work.It starts from the study on the current state of research in the field of pneumatic drives, after which the elaboration of the theoretical study on the mass flow characteristic equations specific to pneumatic drive equipment, including the case of the proportional distributor, follows. In the mathematical modeling part, the equations of the pneumatic linear positioning servomechanism with proportional distributor are described. The presented mathematical model is the basis of the construction of the numerical simulation scheme used to study the performances of the servomechanism.

The results from the numerical simulations are compared with the experimental results obtained on the experimental stand. An experimental identification and connection of the controller used in the control of the servomechanism is thus made.

Chapter II

CURRENT STATE REGARDING THE DEVELOPMENT OF PNEUMATIC ACTUATION SYSTEMS

2.1. Overview

2.1.1 Brief history of the development of the field of pneumatic drives

Pneumatics is the technological field that uses the energy obtained from the compression of air to transform it into energy of practical use.

People have used pneumatic power since ancient times. The first discovery of a device based on pneumatic energy dates back to 429 AD, being an air gun that primitive hunters used to shoot their prey [113].

The first theoretical descriptions of the use of pneumatic energy were written by the Greek mathematician Hero of Alexandria in the first century. He described in his works how his inventions used wind energy to generate mechanical energy to move objects. These applications influenced the German physicist Otto von Guericke to invent in 1600 the vacuum pump that could extract air or gas using air pressure [113]. The Industrial Revolution of the 1800s also led to a great development in the field of pneumatics, pneumatic energy being used especially in the transport, communication and manufacturing industries. [114].

2.1.2 Market trends of pneumatic actuation systems

According to Grand View Research, the pneumatic actuation system market size was valued at USD 30.82 billion in 2022, of which the food industry accounts for 29%. In Fig. 2.1 presents the percentages of the global market of pneumatic actuation systems, depending on the industry used, respectively: pharmaceutical, ceramic, food industry, rubber and plastic industry, cement industry, mining, automotive industry and others [93].

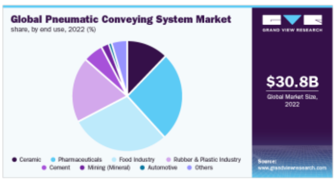

Figure 2.1 Global Pneumatic Actuator Market by Industries Served [93]

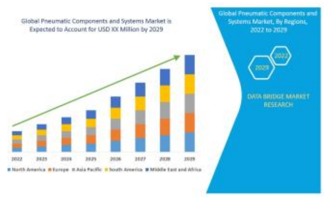

Figure 2.2. Global pneumatic components and systems market growth forecast 2022-2029 [116]

In Data Bridge's market research report on the demand for pneumatic actuation components and systems, we are presented with the fact that the market is expected to grow by 6.6% from 2022 to 2029 [116].

The main industry that will play an important role in this growth is the food industry, due to food safety regulations. In addition, the growing demand for machine safety and operational optimization will provide even more opportunities for the growth of the pneumatic drive components and systems market in the coming years [116]. Figure 2.2 shows the global market growth forecast for pneumatic components and systems in the period 2022-2029.

2.2. Structures of electropneumatic servomechanisms

Servomechanisms, both hydraulic and pneumatic, have seen great development in various industrial automation applications. Numerous specialized works, published in recent years, highlight the new trends and the benefits of using actuation systems with proportional equipment (valves, chokes, distributors).

Pneumatic servomechanisms are systems used for command and control, which can have in their structure:

- on-off solenoid valve;
- proportional distributors;
- pneumatic servovalves.

Distributor control can be analog (or continuous), and digital (or discrete). Likewise, on-off solenoid valves can have PWM (Pulse Width Modulation) signal control.

If in the case of the pneumatic system with a proportional distributor we can have a precise control of the movement of the distributor drawer, also having a linear behavior ensured by the electronic control part of the proportional pneumatic distributor, in the case of pneumatic systems with a solenoid distributor only quick switching can be done starting- stop, without being able to have a control over the movement of the distributor drawer which has intrinsically non-linear behavior [73].

The advantage of actuation systems with solenoid valve is that they are simple and easy to maintain, whereas pneumatic systems with proportional distributors, although they are more expensive and have a complex structure, have excellent static and dynamic performances [73]. Therefore, many of the applications that used pneumatic servo drives with servo valves, have been replaced by proportional distributors.

Due to the advantages they have, such as low cost and clean technology, pneumatic actuators are used in numerous industrial applications such as: actuation of valves used in the energy industry, in water supply, water treatment plants, industrial robots, food industry, haptic system in medical and laboratory equipment, tracking and positioning systems, etc. [33].

2.3. Theoretical research on electropneumatic components

Numerous theoretical studies have been carried out in which an attempt was made to determine a mathematical model for pneumatic systems.

One of these studies was carried out by B. K. Saha, H. Chattopadhyay, P. B. Mandal, T. Gangopadhyay, entitled "Dynamic simulation of a pressure regulating and shut-off valve" [93], in which the authors determined the mathematical model regarding the dynamic behavior of the flow process inside a pressure regulating and closing valve.

The numerical simulations were carried out in this case with the ANSYS-FLUENT software in order to solve the Navier-Stokes equation. With the help of the ANSYS-FLUENT program it was possible to determine the movement of the drawer and its final position after it is deviated from the equilibrium position [93]. The scheme used by the authors in the analysis of the movement of the valve drawer is shown in Fig. 2.3.

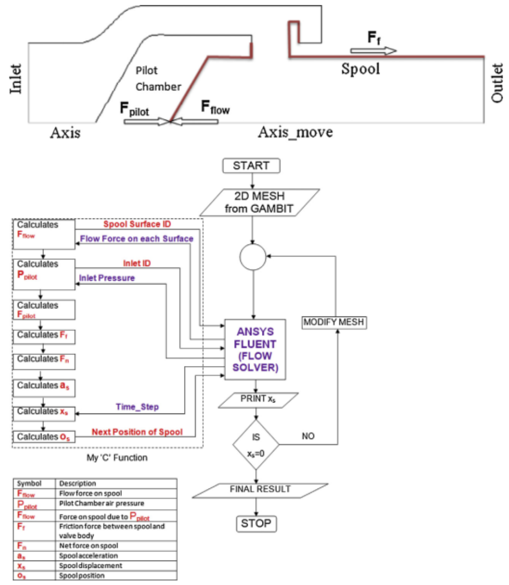

Figure 2.3. Chart for drawer movement analysis [93]

Figure 2.4 shows the transient variation of the forces on the surface of the drawer for the pressure value of 33/31 psi. Initially the valve is forced fully open. When the pressure difference between the inlet and outlet is smaller, the pressure peaks around 410 Pa (Fig. 2.4), and increases to 430 Pa at higher pressure difference [93].

Figure 2.5 shows the drawer position over time, for different valve inlet and outlet pressures [93]. The results of numerical simulations show the behavior of the drawer during the action of the working fluid and provide useful data in the design of such equipment.

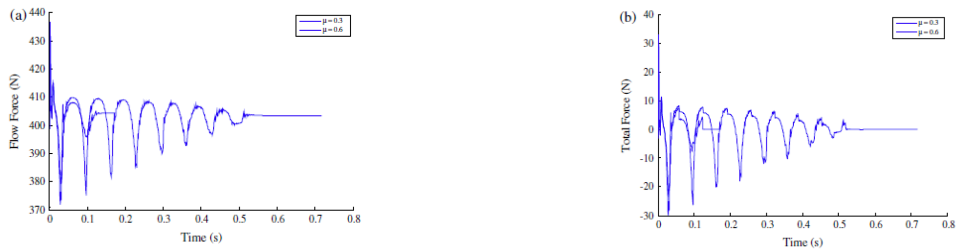

a) b)

Figure 2.4. Transient variation of (a) flow forces and (b) total forces on drawer surfaces at 33/31 psi pressures [93]

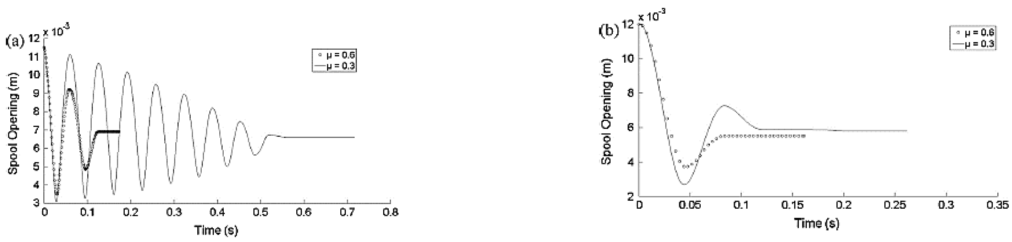

a) b)

Figure 2.5 Drawer movement at pressures (a) 33/31 psi and (b) 39/31 psi [93]

2.4. Experimental research on electropneumatic components

In addition to numerous studies in which the authors presented the results of numerical simulations of mathematical models corresponding to different types of pneumatic components, numerous experimental tests were also carried out to demonstrate the performance of these equipments and to validate the numerical simulation models used.

For example, B. Cui, Z. Lin, Z. Zhu, H. Wang, G. Ma in the paper "Influence of opening and closing process of ball valve on external performance and internal flow characteristics" do experimental research on the dynamics of a ball valves tested at repeated closings and openings to check the sealing of the valve [31].

The experimental tests were carried out on the test stand shown in Fig. 2.6, consisting of a water tank, a control valve, a water pump with variable flow, a flow meter, an input flow control valve and one for upstream and downstream output flow, a ball valve, two pressure sensors and pneumatic test ball valve [31].

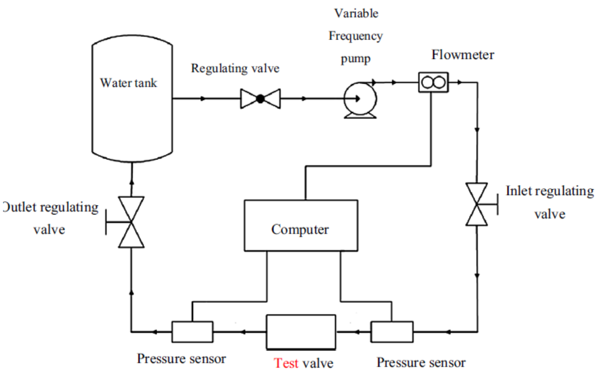

a)

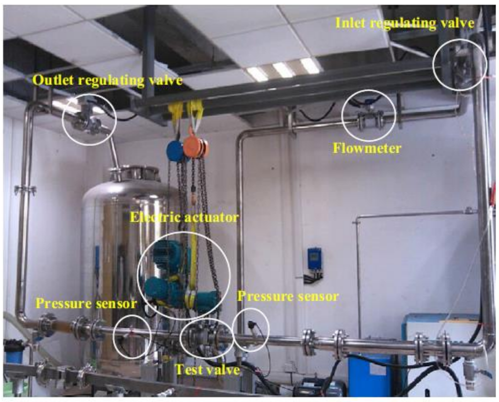

b)

Figure 2.6. Experimental system. (a) Scheme of the experimental system. (b) Experimental system with ball valve [31]

Numerical and experimental results are presented by the authors in figures 2.7 and 2.8.

A good correspondence is observed between the numerical simulation results and the experimental ones for the variation of opening/closing of the valve upstream of the ball valve. The opening-closing intervals considered on each upstream/downstream valve are 20–75%, 20–70%, 20–65% and 20–60% corresponding to 18s, 23s, 34s and 70s, respectively [31].

In this study the ball valve actuation was done electrically, but the same performance was obtained with a pneumatic proportional distributor actuation.

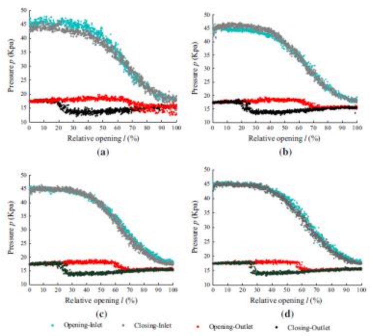

Figure 2.7 Pressure drop variation curves for openings at (a) 18 s, (b) 23 s, (c) 34 s and (d) 70 s [31]

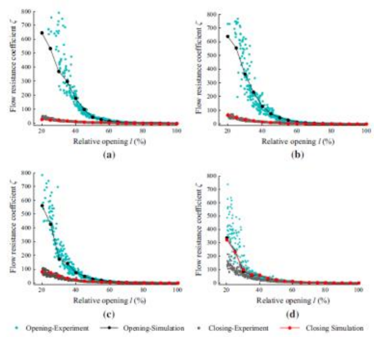

Figure 2.8 Variation of yield strength coefficient for spans at (a) 18 s, (b) 23 s, (c) 34 s and (d) 70 s [31]

2.5. Technological innovations in pneumatic drive applications

As a result of the growing number of vehicles with the internal combustion engine as their propulsion system, with the disadvantage of increasing CO2 emissions, alternatives have been sought to replace this type of propulsion with a less polluting system.

Such a solution was presented in 2002 at the International Vehicle Fair in Paris, where the prototype of a vehicle propelled by a pneumatic engine was presented, which works as a result of the expansion of compressed air. Because it was not possible to obtain a very high autonomy of this type of engine, a hybrid vehicle was created, consisting of a conventional engine and a pneumatic one whose operating principle is shown in the principle diagram in Fig. 2.9.

The mechanical energy produced by the internal combustion engine is transmitted to the compressor which produces compressed air. Compressed air is stored in a compressed air tank. To control the pressure in the tank, a pressure valve is installed, which releases the air into the atmosphere if the pressure in the tank rises above the allowed level [46].

From the tank, the compressed air is transported to the collection pipe where it joins the exhaust gases emitted by the internal combustion engine. To control the amount of compressed air delivered to the collection line, an adjustable pneumatic throttle is mounted between it and the compressed air reservoir [46].

The compressed air together with the exhaust gases reach an air turbine, which drives the wheels of the vehicle [46].

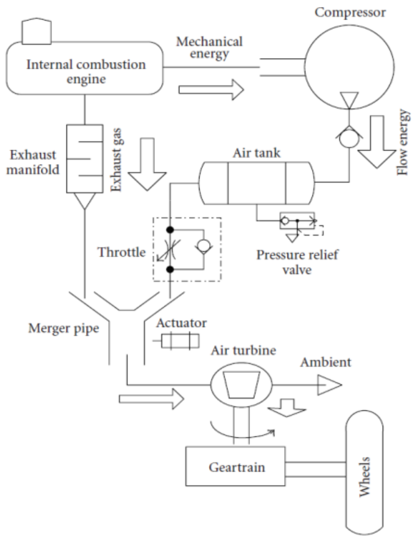

Figure 2.9. Schematic of a conventional/pneumatic hybrid vehicle [46]

As a result of the implementation of this hybrid system, the efficiency of the propulsion system can increase by up to 24%, thus leading to a decrease in fuel consumption and therefore CO2 emissions [46].

EQUIPMENT AND ELECTROPNEUMATIC ACTUATORS

3.1. Overview

Electropneumatic positioning servomechanisms are automatic systems that have in their structure the component elements shown previously in Fig. 1.1 and which, within a pneumatic actuation installation, must harmonize and interact with existing pneumatic sub-systems. That is why, in the present chapter, a brief presentation of the basic elements characteristic of electropneumatic actuation systems is made.

The need to achieve the most precise positioning in various industrial applications has led to the development of numerous drive system structures including pneumatic drives. Pneumatic drive technology is currently tending to replace, where possible, hydraulic and electrical drives [96].

The nonlinearities that dominate the dynamic behavior of these types of servomechanisms have, however, restricted the field of work. And yet, in the specialized literature of the last decade, a constant concern is mentioned in reducing non-linearities, improving static and dynamic performances, and relaunching pneumatic servomechanisms as integral pneumatics systems, "integral pneumatics", in which the command and generation of mechanical work using compressed air is associated with electronic control.

The nonlinearities of the pneumatic actuation systems are given by the compressibility of the working fluid (compressed air), the air mass flow-pressure relationship when the air flows through the holes, the friction effect between the actuator surface and seals, the dead zone from the characteristic of the pneumatic amplifier, the properties of the materials in the structure pneumatic elements [90].

In the 21st century, the development of fieldbus and Ethernet industrial communication technologies brought new solutions in the development of pneumatic components to be used in complex automation schemes.

Table 3.1 mentions the characteristics of pneumatic drives compared to hydraulic and electric drives [117].

Comparison between the characteristics of different types of actions [117] **Table 3.1**

Characteristics	Pneumatic Actuation	Hydraulic drive	Electric drive
Complexity	Simple	Average	Average/ complex
Power developed	Big	Very big	Big
size	Small	Very small	Average
Action Control Mode	Simple valve	Simple valve	Controller
Accuracy	High	High	Very good
Speed	Rapid	Small	Rapid
Acquisition cost	Low	Big	Big
Operating cost	Average	Big	Low
Maintenance cost	Low	Big	Low
Main components	Compressor/ pipelines/energy	Pump/ piping/ power	Energy

Efficiency	Low	Low	High
reliability	Very good	High	High
Maintenance required	Low	Average	Average

3.2. Air properties

The working fluid used in the case of pneumatic drives is compressed air in a gaseous state. It has properties common to liquids, including the fact that it does not have a precise shape, but takes the shape of the enclosure in which it is located. Compared to liquids, gases do not have a well-defined volume. Also, compared to liquids, gases are compressible fluids. Gases are light fluids and less dense than liquids.

Air is composed of 78% nitrogen, 21% oxygen and 1% other gases (e.g. argon or carbon dioxide). Dilution of oxygen with nitrogen makes air much less chemically active than pure oxygen, and is capable of causing spontaneous combustion or explosion; the air comes into contact with petroleum vapors at high temperatures.

Air has a great affinity with water. If not specifically dried, it contains considerable amounts of water vapor, sometimes up to 1% by weight [118].

Table 3.2 shows the properties of air [118].

Table 3.3 shows the advantages and disadvantages of using compressed air [118].

Air properties [118] **Table 3.2**

Air properties	Values
Molecular weight	28.96 kg/kmol
Air density at 15 C and 1 bar	1.21 kg/m^3
Boiling point for 1 bar	191 to -194
Freezing point for 1 bar	212 to -216
Gas constant	286.9 J/kg K

Advantages and disadvantages of compressed air [118] **Table 3.3**

Advantages of compressed air	Disadvantages of compressed air
It is available in unlimited quantity.	It is relatively expensive.
Compressed air is easy to transport through pipes, even over long distances.	Compressed air requires special conditions, without dust or moisture.
It can be stored.	It is not possible to achieve uniform and constant movement of the piston because air is compressible.
It does not pollute, after use it can be released into the atmosphere.	Compressed air is economical only up to certain pressure values. The usual pressure is 7 bar (with a force limited to about 20 to 50 kN). If a force greater than this value is required, the hydraulic system is preferred.

Compressed air is not affected by temperature variations, therefore operation is ensured even in extreme conditions.	The oil necessary to lubricate the equipment, mixed with the compressed air, is discharged together with it into the atmosphere.
It is a clean agent and can be used in industries such as food, pharmaceutical, etc.	Air, due to its low conductivity, cannot dissipate heat as well as hydraulic oil.
The elements used in compressed air operation are simple and have low construction costs.	Air cannot seal clearances of the order of μm between moving parts, unlike the hydraulic system.
It is fast and can easily perform high speed maneuvers.	Problems arise considering that air is not a very good lubricant.
The speeds and forces of the pneumatic elements can be infinitely adjusted.	

3.3. Pressure and flow domains

In the case of pneumatic drives, there are standards that specify the fields of flow rates, pressures, flow diameters and constructive dimensions for the execution elements. In Table 3.4, the constructive elements necessary for the design of pneumatic cylinders according to ISO standards are specified.

Dimensions and tolerances for standard pneumatic cylinders [127] **Table 3.4**

Standard	Piston diameter [mm]	Length of stroke [mm]	Allowable stroke tolerance [mm]
ISO 6432	8,10,12,16,20,25	0…500	+1.5
ISO 15552	32	0…500	+2
	40,50	500…12500	+3.2
	63	0…500	+2
	80,100	500…12500	+4
	125,160	0…500	+4
	200,250,320	500…2000	+5
ISO 21287	20,25	0…500	+1.5
	32,40,50	0…500	+2
	63,80,100	0…500	+2.5

The actuation force of the piston is calculated according to its area, the actuation pressure and the friction force, considered 10% of the pressure force F_p:

$$F = F_p - F_f = p\,A - 0{,}1F_p = 0{,}9 \cdot p \cdot \frac{\pi d^2}{4} \qquad (3.1)$$

where: F is the piston force (N), p- operating pressure (Pa), A- piston area (m^2), d- piston diameter (m), F_f – friction force ≈ $10\% \cdot F_p$ (N), F_p pressure force (N).

3.4. Pneumatic equipment

Pneumatic drives are used in industrial automation, due to their advantages (Table 3.1) over other automation systems.

Pneumatic actuation systems are divided into two categories:

- ✓ pneumatic actuation elements for flow and pressure regulation;
- ✓ pneumatic execution elements.

Figure 3.1 shows the specific component elements of a proportional pneumatic distributor [5].

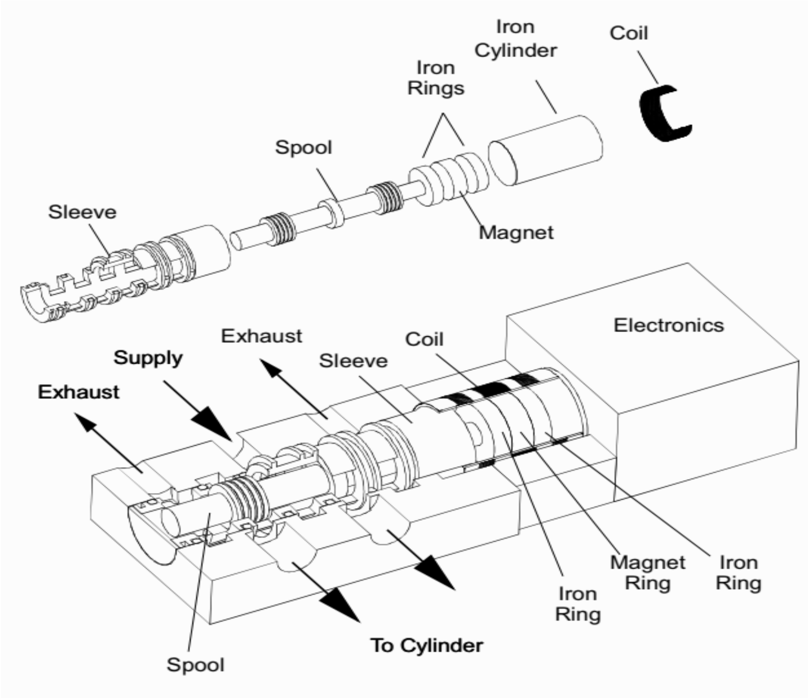

Figure 3.1. Proportional distributor. Constructive elements [5]

The performance criteria specific to proportional distributors in stationary mode are [5]:

- air losses (represented by the air flow passing through the distributor when the drawer is in the zero position and all the distribution paths are blocked;
- flow amplification (represented by the slope of the mass flow characteristic vs the input signal. It is a measure of the sensitivity of the mass flow to changes in the input signal);
- hysteresis (which occurs due to friction and temporary deformations of the elastic components in the construction of the distributor, which causes different values of the output quantity from the distributor to appear for the same command signal);
- pressure amplification (represented by the slope of the differential pressure in relation to the input signal at the origin).
- The dynamic performance criteria specific to proportional distributors are [5]:
- the frequency response (which is given by the Bode plot, i.e. the representation of the gain and phase of the output signal in response to different sinusoidal input signals, with independently variable frequency). Due to non-linearities this response depends on the amplitude of the input signal. At the cutoff frequency the output signal is 3 dB lower than at a very low frequency;
- step signal response (which represents the displacement of the cylindrical drawer when a step is applied to the input from 0 to 100% or from 20% to 80%, tracking system response time and damping.

The following specific technical characteristics of proportional distributors are specified in the specialized literature [5]:

- the flow range covered is 100÷2000 l/min (ANR) with an error margin of ± 10%;
- the air flow rate lost through seals is 1.3 - 5% of the nominal flow rate under conditions of 6 bar pressure and blocked outlet;
- pressure amplification: it is appreciated by a displacement of the distributor drawer of less than 3% starting from zero to obtain 80% of the maximum pressure;
- hysteresis < 0.4% relative to the maximum stroke of the distributor drawer and having the reaction link on the drawer;
- the cut-off frequency, -3dB at 60 Hz for the maximum amplitude of the distributor with the nominal flow of 2000 l/min, 320 Hz at ± 5% of the amplitude for the distributors with 100 l/min;
- the bandwidth is 80÷150 Hz at 90°;
- the response time of the distributor for 100% drawer displacement is below 12 ms, regardless of the distributor flow and for the drawer travel from 20% to 80% of the drawer displacement is 3 ms for distributors with a nominal flow of 100 l/min, respectively 5.2 ms for those with 2000l/min.

3.5. Electropneumatic drives

In this sub-chapter, types of pneumatic actuation schemes (closed loop and open loop) presented in the studied references are presented. Some schemes are also accompanied by the electric control schemes of the electromagnets in the pneumatic distribution apparatus, without which the operation of the actuation scheme is not possible. All actuation diagrams show the execution element and compare the actuation of an open-loop versus closed-loop actuator. Electropneumatic servomechanisms are actuation systems that operate with a control loop.

Chapter IV

MATHEMATICAL MODELING OF PNEUMATIC SERVOMECHANISMS WITH LINEAR ACTUATORS

4.1. Overview

Pneumatic actuation systems have been developed since the first decades of the 20th century, but the year 1956 marks the beginning of pneumatic system control technology through the work of Shearer J. L. "Study of Pneumatic Processes in the Continuous Control of Motion With Compressed Air, Parts I and II", Trans. of the ASME, Feb. 1956, pp.233-249, 1956. In the following decade, Borrows develops the "switch" control technology, Burrows C. R. "Fluid Power Servomechanisms", 1972, Ed. Butler & Tanner, and Professor W. In 1979 he developed the electropneumatic servovalves. In the 1980s, proportional pneumatic equipment began to be developed [61,75,74].

Electropneumatic positioning systems, as a rule, use in their structure pneumatic servovalves characterized by special performances ([134] hysteresis ≤ 4%; symmetry of the static flow characteristic ≤ 10% at nominal command current; response time 8ms) but at prices of high cost.

The purpose of the current chapter is to present the standard mathematical model associated with an electropneumatic linear positioning servomechanism. Also, mentions are made of the non-linearities characteristic of these systems and the method of controlling and reducing the influence of the non-linearities on the performance of the servomechanism by using an appropriate regulator.

4.2. Air flow through nozzles and holes

Unlike the flow of liquids through nozzles and holes, where the liquid is considered an incompressible fluid, in the case of gases, their compressibility property is taken into account. Thus, by applying pressure to a mass of gas, it is compressed and the density of the gas changes. On the other hand, considering the thermodynamic properties, the temperature will also change.

Considering an ideal gas, with a given mass, the equation of state of the gas is known:

$$p = \rho R T, \tag{4.1}$$

with p gas pressure (Pa), ρ density (kg/m^3), R[1] air constant (J/(kg·K), T temperature (K). In the case of isothermal transformations, the equation of state becomes $\frac{p}{\rho}$ =const.; for the adiabatic transformation, $\frac{p}{\rho^k}$ =const., with k adiabatic exponent and $k = 1{,}4$ for air. In the polytropic flow of a gas mass, $\frac{p}{\rho^n}$ =const., with n polytropic coefficient and $1 < n < k$.

Consider the schematic representation, Fig. 4.1, of the flow of a gas through an orifice[2]. Noted

[1] For air with relative humidity 65%, R=288 J/(kg·K), T=293.15 K, p=100 kPa, according to ISO 6358.

[2] Holes are defined as openings of various geometric shapes, with their technical use in measuring equipment (eg Diaphragm). Nozzles are defined as short pipes attached to an orifice for directing a jet of fluid. Their functional role in installations is to control the flow direction. A major difference between holes and nozzles is given by the technological processing: the holes have sharp edges; nozzles have rounded edges, which causes lower energy losses when crossing the nozzle, so a higher flow coefficient [5].

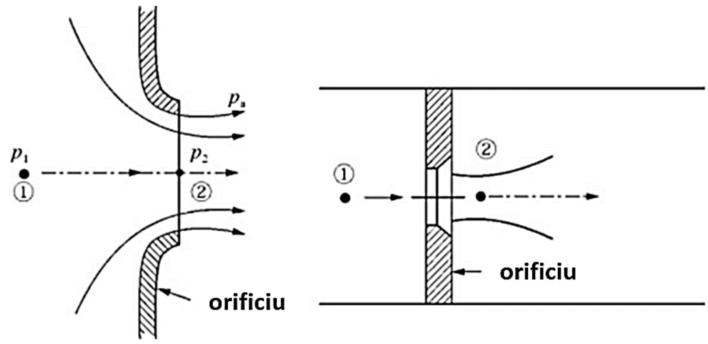

a) b)

Figure 4.1. Flow through holes: a) flow from the inside of a container to the outside; b) flow through the hole placed inside a pipe [110]

The gas pressure at the entrance to the hole is marked with "1", respectively at the exit with "2". If the gas exit is at atmospheric pressure, the notation is p_a.

The following working assumptions are made:

- The gas through the orifice is an ideal gas and the state parameters of the gas in the flow process do not change with time;
- From a thermodynamic point of view, the flow of gas through the orifice is an adiabatic process, which means that when the gas passes through the orifice, there is not enough time to exchange heat with the outside;
- When the gas passes through the orifice, the flow velocity in the upstream (inlet) side is much lower than that in the downstream (exit) side;
- When the gas passes through the orifice, the gas flow coefficient C_d is constant.

Considering the effective area of the orifice A, and taking into account the phenomenon of contraction when flowing through the orifice and of pressure loss, the (theoretical) gas mass flow rate at the exit of the orifice is determined:

$$G = \rho_2 A u_2 = A\rho_1\sqrt{kRT_1}\cdot\sqrt{\frac{2}{k-1}\cdot\left[\left(\frac{p_2}{p_1}\right)^{2/k}-\left(\frac{p_2}{p_1}\right)^{(k+1)/k}\right]}. \tag{4.2}$$

Given equation (4.1) and substituting $\rho_1 = \frac{p_1}{R\cdot T_1}$ it is obtained:

$$G = A\frac{p_1}{\sqrt{RT_1}}\cdot\sqrt{\frac{2k}{k-1}\cdot\left[\left(\frac{p_2}{p_1}\right)^{2/k}-\left(\frac{p_2}{p_1}\right)^{(k+1)/k}\right]}. \tag{4.3}$$

The flow from formula (4.3) is also characteristic of nozzles that have flow coefficients very close to the value 1. For example in Fig. 4.2 presents several forms of holes with the specified flow coefficient C_d. It is observed that for the first type of hole, with rounded edges specific to nozzles, $C_d = 0{,}98$.

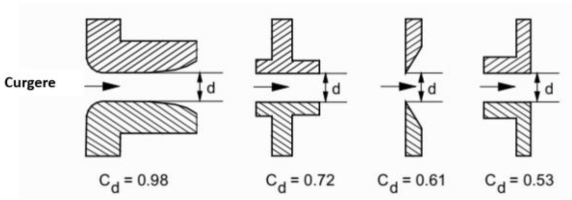

Figure 4.2. Different orifice shapes and corresponding flow coefficients [5]

It is known that due to the contraction of the air jet when flowing through the hole, a contraction coefficient C_c appears which, together with the velocity coefficient C_v forms the flow coefficient $C_d = C_c \cdot C_v$. In these conditions, the mass flow rate through an orifice (with sharp edges) is:

$$G = C_d \cdot A \cdot \frac{p_1}{\sqrt{RT_1}} \cdot \sqrt{\frac{2k}{k-1} \cdot \left[\left(\frac{p_2}{p_1}\right)^{2/k} - \left(\frac{p_2}{p_1}\right)^{(k+1)/k}\right]}. \tag{4.4}$$

where: C_d is the gas flow coefficient.

In Fig. 4.3 the mass flow of air through the nozzle (marked "Ga") was represented graphically with formula (4.3) and the mass flow through the hole (marked "Go") was represented with formula (4.4) considering $C_d = 0{,}61$. On the same graph, the Mach[3] number, variations were also represented, in the two situations, respectively nozzle and orifice, to highlight the two flow regimes highlighted by the graph. For Ma<1 the flow is subsonic and on the graph it can be seen that the part to the right of the point $\left(\frac{p_2}{p_1}\right)_{cr} = 0{,}5283$ corresponds to this condition. For Ma>1 we will generically call sonic flows [110] and they are found to the left of the critical pressure ratio. Also, it is observed that in the case of the nozzles, the values of the Mach number enter the supersonic range of flow (Ma<5).

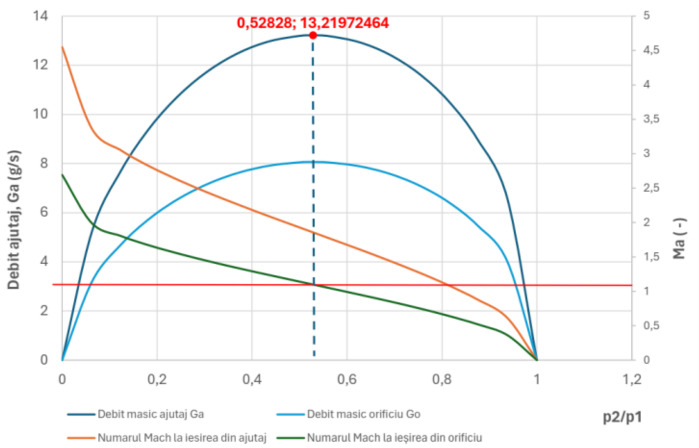

Figure 4.3. Pressure-mass flow curve for nozzle and orifice

In [5] it is specified that if Ma<0.3 the gas density varies by less than 5% and the flow can be considered incompressible.

[3] Mach number highlights the types of flows by relating the speed of the source (flow medium) to the speed of sound in the flow medium.https://ro.wikipedia.org/wiki/Num%C4%83r_Mach

4.3. Mass flow characteristic through variable area orifices

Also, in Fig. 4.3 the pressure-mass flow curve was represented in the case of the holes compared to the case of the nozzles. The difference between the two representations is also visible from a physical point of view, very important if we also refer to the representation of the Mach number as a function of pressure. Coupled with the observation in [5] that the difference in flow velocity at the opening of the distributor drawer is 35% of the speed of sound in air, we must understand the importance of the flow coefficient C_d in the description of the equations. Also, we should mention that the mass flow equations through the orifice or nozzle are valid for high Reynolds numbers. For example, for $\left(\frac{p_2}{p_1}\right)_{cr} = 0{,}5283$ at the maximum orifice flow rate of 8.064 g/s (for the considered example) $Re = 223359{,}83$ is obtained considering the kinematic[4] air viscosity $\nu = 1{,}5356 \cdot 10^{-5}$ m^2/s.

The flow coefficient C_d depends on the geometric shape of the hole, Fig. 4.2, but also by the upstream-downstream pressure ratio, according to the relationship [5]:

$$C_d = 0{,}8414 - 0{,}1002\frac{p_2}{p_1} + 0{,}8415\left(\frac{p_2}{p_1}\right)^2 - 3{,}9\left(\frac{p_2}{p_1}\right)^3 + 4{,}6001\left(\frac{p_2}{p_1}\right)^4 - 1{,}6827\left(\frac{p_2}{p_1}\right)^5. \tag{4.5}$$

In Fig. 4.4 represents the variation of the flow coefficient using relation (4.5) and the differences that appear within the flow coefficient if we consider the first 2, or 3, respectively 4 terms compared to the entire degree 5 polynomial used in the description of this coefficient. From the graphic representation it can be seen that for the situation in which we consider only the first 4 terms, C_d also has negative values, which from a physical point of view is not possible because $C_d = C_c \cdot C_v$ or $C_d = G_{real}/G_{teoretic}$. Also, for C_d calculated with the first 3 terms, the values obtained are greater than 1, which would mean that the real flow rate is higher than the theoretical one, which is physically impossible. The only variant worth considering is the one in which the first 2 terms of the polynomial expansion in (4.11) are considered. In Fig. 4.5 compares the variation of the flow coefficient in degree 5 polynomial form compared to the linear form (the first 2 terms).

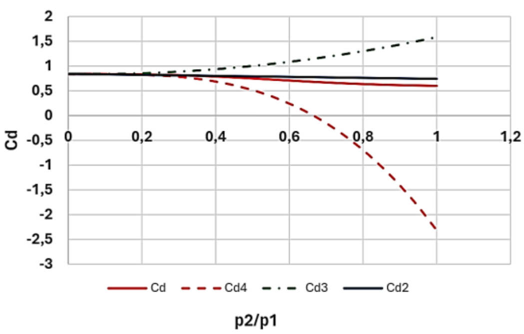

Figure 4. 4. Variation of the flow coefficient for the orifices of pneumatic distributors and comparison for the approximation with polynomials of degree 3, 2 and 1

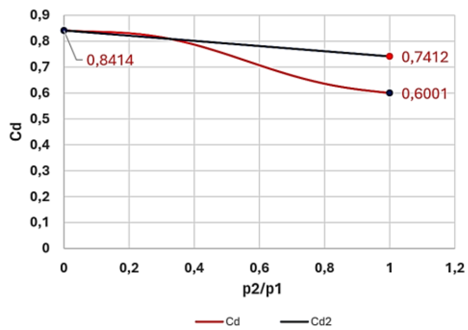

Figure 4.5. The variation of the flow coefficient for for the approximation with polynomials of degree 5 and 1

[4] Air viscosity was calculated using the formula [37] $\nu = 9{,}95182 \cdot 10^{-11}T^2 + 3{,}55322 \cdot 10^{-8}T - 3{,}60844 \cdot 10^{-6}$, where T is the air temperature, $T = 293{,}15$ K.

Considering the previous observations, in Fig. 4.6 represents the flow characteristic of the orifices of a distributor considering the sonic character of the flow for $\frac{p_2}{p_1} \leq 0{,}5283$ and subsonic for $\frac{p_2}{p_1} > 0{,}5283$.

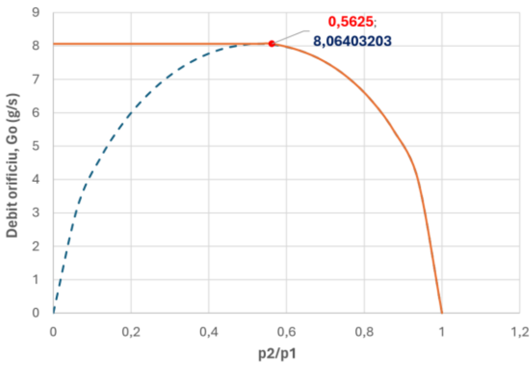

Figure 4.6. The flow characteristic of a distributor orifice

The ratio $\frac{p_2}{p_1} = 0{,}5283$ results in a critical pressure downstream of the hole, respectively at the outlet, $p_{2cr} = 0{,}5283 p_1$ or which the critical speed is equal to the speed of sound because $Ma = 1$, Fig. 4.3.

In the case of pneumatic equipment, the flow area is variable. Considering the area of the hole A and the pressure at the hole entrance $p_1 = p_s = const.$ and outlet pressure p_2, the mechanical work of the gas when flowing through the orifice is [110]:

$$N = \int_{p_e}^{p_{10}} G dp_2 = \int_{p_e}^{0{,}5283 p_{10}} G dp_2 + \int_{0{,}5283 p_{10}}^{p_{10}} G dp_2. \quad (4.6)$$

So, when the pressure ratio is $0{,}5283 \leq \frac{p_2}{p_1} \leq 1$ the gas flow is subsonic and the mass flow is in a non-linear relationship with the pressure ratio $\frac{p_2}{p_1}$. When $0 \leq \frac{p_2}{p_1} < 0{,}5283$ the gas flow is sonic and the mass flow has its maximum value. In this situation the flow is called "blocked flow" and the flow reaches saturation.

The mechanical work of air flowing through an orifice is the area of the pressure-flow characteristic in the sonic and subsonic flow domain.

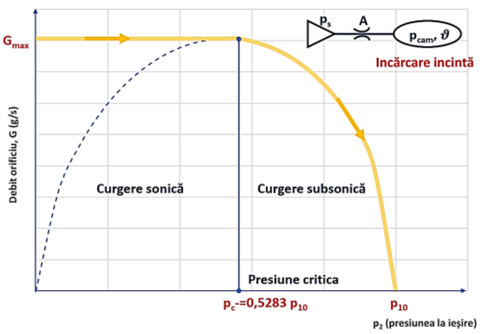

Figure 4.7. Pressure-flow curve at the orifice exit ($p_1 = p_s = const.$)

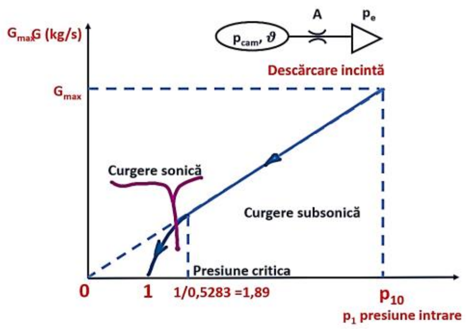

Figure 4.8. Pressure-flow curve at the inlet of the orifice ($p_2 = p_s = const.$)

In Fig. 4.8 represents the pressure-flow characteristic for the entry of the fluid into the area hole A as specified in the diagram in the upper right corner of the characteristic, when the volume enclosure ϑ is discharged through the hole at the pressure p_{cam}.

The mechanical work of the gas entering the chamber of volume ϑ is 2 times greater than the mechanical work of the gas leaving the chamber through the same orifice [110].

4.4. Numerical simulations on the dynamic behavior of proportional distributors

Starting from the bibliographic reference [77] in which the authors make an experimental identification of the air flow through a proportional distributor of the FESTO type, respectively MPYE-5-1/8HF-010B, we reconstructed by numerical simulation the dynamic behavior of this type of distributor and I compared the results with those in the article. Corrections determined experimentally by the authors of the article were used in the simulation model.

I mention that I used the same type of distributor because also in the numerical and experimental research within the thesis I used the same type of proportional pneumatic distributor DPP [19, 21, 22, 23, 24, 25, 26, 92].

The authors of the article determined by measurements the areas of the 5 flow holes of the DPP. The distributor is connected on the stand to one volume chamber ϑ that practically replace the chambers of a pneumatic actuator. Also, it is noted that the way of working proposed by the authors of the article is very close to the observations made in the discussions of figures 4.7 and 4.8.

For the effective working area, the authors use the formula [77]:

$$A_{eff} = A_m \frac{\left(1-\left(\frac{u-U_s}{U_0-U_s}\right)\right)}{\alpha_2 p_s{}^2+\alpha_1 p_s+\alpha_0} \tag{4.7}$$

where A_{eff} is the effective flow area, A_m the measured area, u control voltage of DPP, U_0 correction voltage, U_s voltage at which the distributor drawer is in the middle position, p_s supply pressure, $\alpha_0, \alpha_1, \alpha_2, C, D$ experimentally determined quantities.

For the data provided by the article, based on the formula in (4.7), the correction coefficients of the effective flow area were graphically represented Fig. 4.9.a and the variation of the effective area Fig. 4.9.b to different control signals u.

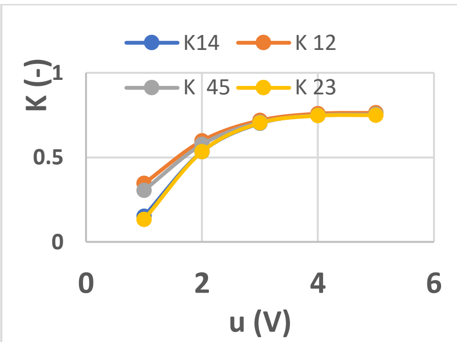

a)

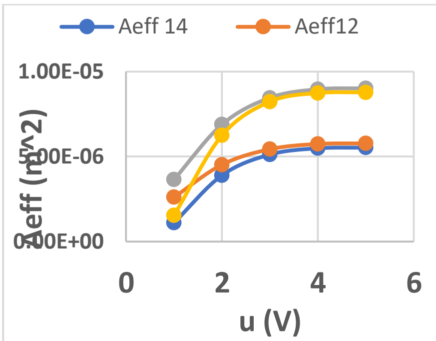

b)

Figure 4.9. Correction factor variation (a) and variation A_{eff} (b) at different values of the control voltage u

The proposed numerical simulation scheme is represented in Fig. 4.10 and the values used in the simulations are mentioned in table 4.1 and table 4.2.

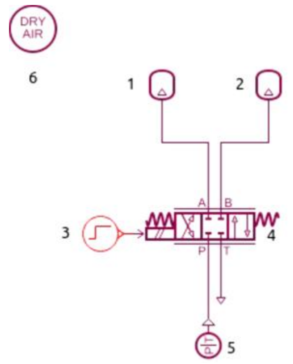

Figure 4.10. Numerical simulation scheme: 1.2 Tanks; 3-command signal; 4- proportional distributor 4/3; 5- gas supply source at a pressure of 8barA; 6- the type of gas used

Numerical values used in the simulation **Table 4.2**

	Charging		**Discharge**		**Figure**		**Coefficient C_d**	**Representation type**
Parameter	**Orifice P,A**	**Orifice P,B**	**Orifice B,T**	**Orifice A,T**		**Step signal (V)**		
Orifice area [mm^2]	7.30	7.57	11.96	11.71	4.11	1;-1	0.82	Pressure at port 1
	7.30	7.57	11.96	11.71	4.12	1;-1	0.82	temperature at port 1
	7.30	7.57	11.96	11.71	4.13	1;-1	0.82	enthalpy flow rate at port 1 [J/s]
	7.30	7.57	11.96	11.71	4.14	1;-1	0.82	mass flow rate at port 1 [g/s]
	7.30	7.57	11.96	11.71	4.15	1;-1	0.82	mass of gas in chamber [g]
	7.30	7.57	11.96	11.71	4.16	1;-1	0.82	pressure at port A for PPD [barA]
	7.30	7.57	11.96	11.71	4.17	3;-3	0.82	presiune port 1
	7.30	7.57	11.96	11.71	4.18	3;-3	0.82	ports to flow area
	7.57	7.57	7.57	7.57	4.19	1;-1 2;-2 3;-3 4;-4 5;-5	0.82	pressure at port 1 avand DPP cu orificiu simetric
	7.30	7.57	11.96	11.71	4.20	1;-1 2;-2 3;-3 4;-4 5;-5	0.82	control step signal

In Fig. 4.11 compares the results of the numerical simulations above, performed with the AMESim program, compared to the results of the numerical simulations from reference [77] performed by the authors in MATLAB-Simulink. The results are comparable. It is observed that the big differences are in the case of a control quantity of 1 V (Fig. 4.11.a). At larger command sizes, u=2 V, the differences are very small.

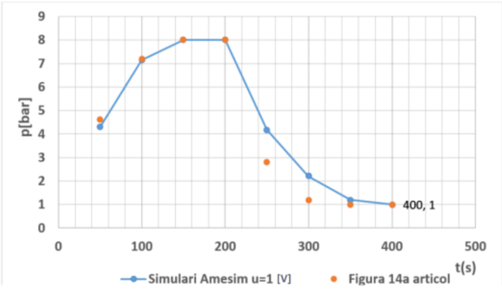

a)

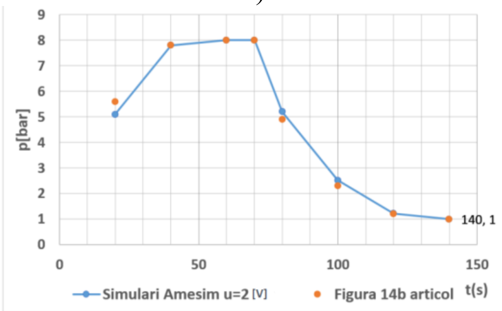

b)

Figure 4.11. Comparison between the results of numerical simulations from reference [77] done in MATLAB-Simulink and those done by the author in AMESim: a) command size u=1 V; b) command quantity u=2 V

The comparative study based on the experimental and numerical results from [77] highlights the following aspects:

- Proportional pneumatic distributors in series production do not have identical control ports. Moreover, the manufacturer specifies that the distributors used in pneumatics have a slight negative cover of the drawer, with values that can be between 5 and 25 μm [42].
- Proportional pneumatic distributors in series production need an experimental identification to determine the areas of the control holes but also the flow coefficient. These quantities are very important in the description of the mathematical model of a pneumatic servo drive because they are present in the flow-pressure characteristic of the DPP.
- From the results of the experiments disseminated in [77] but also from the numerical simulations made by the author, the importance of the value of the flow coefficient C_d is emphasized.

From the bibliography reviewed for the development of this topic, we noted that the FESTO MPYE-5-1/8 construction distributor was the subject of many research and application development topics, respectively [4, 61, 75, 77, 85, 86, 87, 103]. The static and dynamic characteristics of these DPPs explain the interest shown by the scientific community [146].

4.5. Nonlinearities in the operation of electropneumatic servomechanisms

Studies on the performance of pneumatic positioning systems have highlighted the special influence that proportional pneumatic distributors have, respectively their static and dynamic characteristics, on the positioning error and their dynamics.

From the previously presented, the deeply non-linear character of the pneumatic distributors was observed due to the compressibility property of the air and the flow through the distributor openings. Added to these are the frictional forces that appear when the distributor drawer moves, but also the magnetic properties of the materials used in the electro-mechanical converter part of the distributor [4, 56, 76, 77, 95].

The most well-known non-linearities specific to pneumatic distributors are the dead zone (Fig. 4.12.a), the hysteresis (Fig. 4.12.b) and the variation of the flow coefficient Cd presented previously

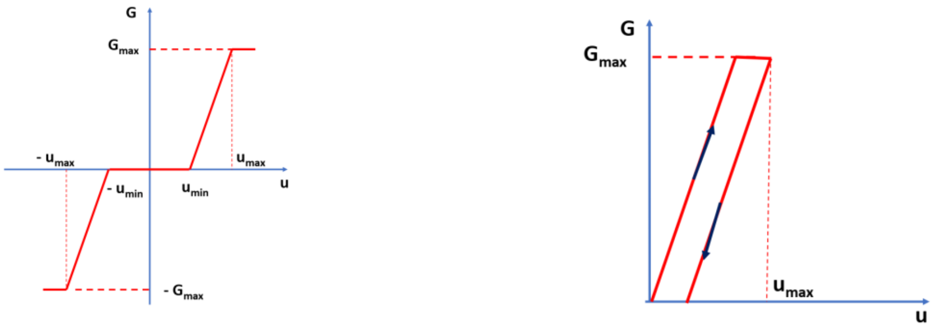

a) b)

Figure 4.12. Non-linearities specific to proportional pneumatic distributors: a) dead zone; b) hysteresis

The presence of frictional forces, both when moving the distributor drawer and the piston of the pneumatic actuator, contributes to the manifestation of non-linearities such as hysteresis and dead zone. Physically, but also mathematically, the friction force has a complex representation, it has both a static component and a viscous dynamic component. In Fig. 4.13 shows the variation of the friction force.

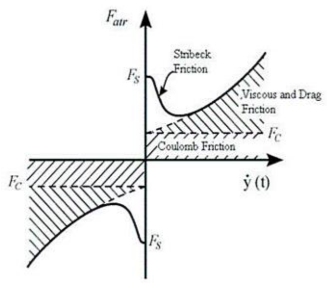

Figure 4.13. Representation of friction force with specification of components [51]

Corresponding to this representation is the associated mathematical model [51]:

$$F_{ss}(v) = sign(v)\left[F_C + (F_S - F_C)e^{-\left(\frac{v}{V_S}\right)^2}\right] + b * v \tag{4.8}$$

where: v is the velocity, F_C the Coulomb friction force, F_S the static friction force, V_s Stribeck velocity, b the coefficient of viscous friction.

Usually, the non-linearities in the mechano-electropneumatic control system can be compensated using different types of regulators (controller) in the structure of the servomechanism.

In Fig. 4.14 shows how, using a modified PVA (proportional plus velocity plus acceleration) controller for friction force compensation, a good operation of the pneumatic actuator is obtained which must develop a force F_{max} even in the range of displacement of the distributor drawer where the dead zone is indicated.

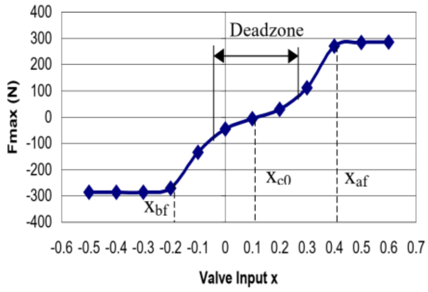

Figure 4.14. Variation of the actuation force of an actuator by controlling the frictional force [76]

Therefore, knowledge of the specific nonlinearities of electropneumatic positioning servomechanisms is particularly important for the description of the mathematical model associated with the system. In turn, the mathematical model is useful in designing the associated regulator (or controller).

4.6. Control methods in pneumatic positioning systems

In the block diagram in Fig 1.1, characteristic of a pneumatic positioning system, the element called controller or regulator connects the reference elements, the reaction link of the system and the command of the electropneumatic amplifier, respectively the proportional pneumatic distributor. In other words, the controller is the command and control element within the system. Regardless of the nature of the DPP command, continuous-analog or discrete-digital, the controller is designed in such a way as to ensure the performance of the tracking system (error and stability) by compensating the nonlinearities in the system.

For pneumatic actuators the most used controllers are the PVA type, i.e. Piston Speed Acceleration, or in other words PID, proportional-derivative-integral. In this situation the control is a position-velocity-acceleration function. In Fig. 4.15 shows the structure of such a controller with the constants K_P, K_D, K_I (proportional-derivative-integrator) hence the name PID controller.

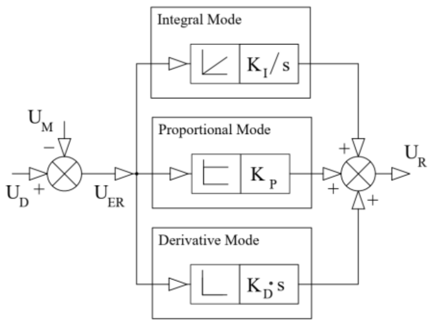

Figure 4.15. Block diagram of a controllerPID [56]

The control function associated with a PID controller is [56]:

$$U_R = K_P \cdot U_{ER} + K_I \int U_{ER} dt + K_D \dot{U}_{ER}. \tag{4.9}$$

The control signal $U_C = K_{PA} \cdot U_R$ is applied to the input of the DPP, and K_{PA} s an amplification factor. The difference $U_{ER} = U_D - U_M$ is the signal error between the reference (desired) input and the measured output signal. Also, the quantity U_R is the quantity that comes out of the controller to be applied to the input of the pneumatic amplifier [56].

PID control can be realized analogically and digitally with the mention that a proportional controller is specific to simple positioning systems [4] without interaction with system disturbing quantities.

When it is desired to optimize the tracking system and improve its performance in the case of different types of applications, the design of the controller is very different from the PID model. Thus, since the first controllers applied to pneumatic servo systems [61], the types of controllers have diversified and the algorithms used for their programming have evolved. Various fuzzy control techniques have been developed and implemented (e.g. fuzzy single input controller for hysteresis compensation [4]), control using adaptive neural networks and metaheuristic optimization techniques [19] (e.g. particle swarm optimization - PSO Particle Swarm Optimization).

It should be emphasized that the methods of designing the controller and designing the programming algorithms for their optimization are adapted to the applications they serve and the operating conditions. So there is no standard method of application.

The error value for the simulation cases from Fig. 4.27, [91] **Table 4.3**

Controller	**Error**
ILC	$2{,}6 \times 10^{-5}$
PID	$3{,}3 \times 10^{-4}$
IT2 T-S fuzzy	$3{,}8 \times 10^{-4}$
T-S fuzzy obs.	$9{,}2 \times 10^{-4}$

4.7. The mathematical model associated with the electropneumatic servomechanism

From the abundant bibliography disseminated, it has been observed that, in general, the concerns of the academic community regarding electro-pneumatic positioning servomechanisms are directed towards the design and optimization of the controller used in the positioning system.

It is known that the design of a controller is based on the knowledge of the mathematical model associated SEPP (proportional electropneumatic servomechanism) of positioning under the conditions of the given application, or under the general conditions of the control structure. Therefore, all the articles, in the reviewed bibliography, which develop the subject of designing/optimizing a controller for a given positioning system, described the associated mathematical model.

In general, there is a "standard" mathematical model in which the nonlinear mathematical model is presented, but there are also often linearized mathematical models described according to the state variables, which brings the system closer to the design methodology of a controller.

In the following, we first present the "standard" mathematical model used in references [53, 106, 107, 108], a model that describes the pneumatic positioning system with the elements shown in the block diagram in Fig. 2.1.Pentru scrierea modelului matematic se au în vedere următoarele ipoteze de lucru [67, 99]:

- ✓ The working fluid is air considered a compressible fluid and an ideal gas for which the thermal equation of state (4.1) is valid;
- ✓ The working pressure is constant p_s=const. and the working temperature as well, T_s=const.
- ✓ The outlet pressure to the atmosphere is the atmospheric pressure;
- ✓ Environmental conditions are constant;

- ✓ The temperature in the chambers of the pneumatic actuator is constant;
- ✓ Air losses between the chambers of the pneumatic actuator and between the chambers and the outside environment are neglected;
- ✓ The switching dynamics of the distributor is neglected because the bandwidth of the DPP is typically greater than 100 Hz [75];
- ✓ An adiabatic system is considered between the positioning system and the environment.

The mathematical model of the pneumatic linear positioning system consists of the pneumatic amplifier, in the present case a DPP, an execution element, namely a pneumatic actuator, and a linear displacement transducer that closes the feedback loop. The reference, signal comparison and controller are in an electronic block separate from the mechanical-pneumatic system.

In Fig. 4.16 presents the positioning system whose mathematical model is detailed below.

The associated mathematical model is described by nonlinear differential equations that come from the following laws of physics:

- ➢ The first law of thermodynamics;
- ➢ Ideal gas equation;
- ➢ Continuity equation;
- ➢ Mass flow equation through an orifice;
- ➢ Newton's second law of motion.

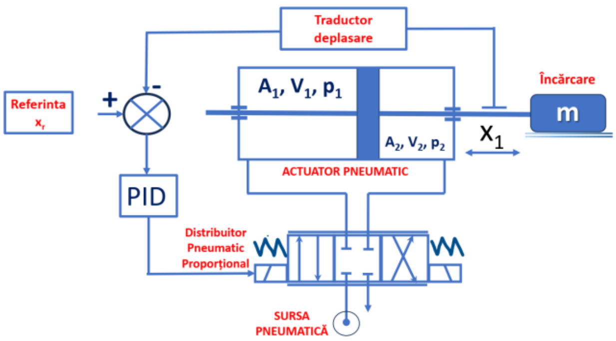

Figure 4.16. Schematic of the modeled pneumatic positioning servo system

The following notations were used in writing the mathematical model:

x_1 pneumatic actuator piston displacement;

x_2 piston travel velocity;

x_3 the pressure in the active chamber of the piston, the upstream pressure;

x_4 the pressure in the passive chamber of the piston, the downstream pressure;

x_5 displacement of the proportional distributor drawer;

p_s supply pressure;

b coefficient of viscous friction;

m inertial mass;

$A = A_1 = A_2$, the active surface of the piston;

F the disturbing force;

F_f friction force;

$V = V_1 = V_2$, the volume of the actuator chambers;

$k = 1{,}4$ adiabatic coefficient;
$R = 287$ J/kg · K, universal gas constant;
$T_s = 293$ K, air temperature from the compressed air source;
C_d flow coefficient;
$w = w_1 = w_2$, distributor hole width;

$$C_0 = \sqrt{\frac{k}{R} \cdot \left(\frac{2}{k+1}\right)^{(k+1)/(k-1)}} = 0{,}040418\,;$$

$$C_r = \left(\frac{2}{k+1}\right)^{\frac{k}{k-1}} = 0{,}52828;$$

$$C_k = \sqrt{\frac{2}{k-1}\left(\frac{k+1}{2}\right)^{\frac{k+1}{k-1}}} = 3{,}864;$$

K_P proportional controller amplification constant P;
K_T time constant of the transducer;
τ time constant of DPP;
p_a atmospheric pressure..

The mathematical model is built for a symmetrical actuator, as noted above $A = A_1 = A_2$ and $V = V_1 = V_2$. Also, all communication ports of the DPP are equal and have the same rectangular shape of width w.

Considering the assumption made to have constant temperature in the pneumatic actuator chambers and no heat exchange between the positioning system and the environment, we can consider $T_s = T_1 = T_2$.

Under these conditions, for the last case given as an example, the equations of the mathematical model can be written:

$$\dot{x}_1 = x_2 \tag{4.10.a}$$

$$\dot{x}_2 = -\frac{b}{m}x_2 + \frac{S}{m}(x_3 - x_4) - \frac{F_f}{m} - \frac{F}{m} \tag{4.10.b}$$

$$\dot{x}_3 = \frac{-kx_2x_3A + R\sqrt{T_s}C_dC_0wx_5 \cdot x_3C_k\sqrt{\left[\left(\frac{p_a}{x_3}\right)^{\frac{2}{k}} - \left(\frac{p_a}{x_3}\right)^{\frac{k+1}{k}}\right]}}{V + Ax_1} \tag{4.10.c}$$

$$\dot{x}_4 = \frac{-kx_2x_4A + R\sqrt{T_s}C_dC_0wx_5 \cdot p_sC_k\sqrt{\left[\left(\frac{x_4}{p_s}\right)^{\frac{2}{k}} - \left(\frac{x_4}{p_s}\right)^{\frac{k+1}{k}}\right]}}{V - Ax_1} \tag{4.10.d}$$

$$\dot{x}_5 = K_P \cdot \left(U_{ref} - K_Tx_1\right) - \frac{1}{\tau}x_5 \tag{4.10.e}$$

From the above, it can be seen that the mathematical model associated with the operation of a linear electropneumatic servomechanism, written in the previously formulated working hypotheses, is a non-linear model formed by a system of ordinary differential equations with a number of five unknowns associated with the system. If the friction force F_f is also taken into account in the description of the mathematical model, the degree of complexity in the analytical solution of this problem exceeds the possibilities of solution within the present thesis. The topic is very interesting from a mathematical point of view and deserves to be developed in a separate paper.

The following chapter presents such dedicated numerical programs and presents the results of numerical simulations for the electropneumatic linear positioning servomechanism studied in the thesis.

Chapter V

NUMERICAL SIMULATIONS TO DETERMINE THE PERFORMANCE OF THE ELECTROPNEUMATIC SERVO-MECHANISM WITH PROPORTIONAL DISTRIBUTOR

5.1 Overview

The mathematical model presented in the previous chapter, for modeling the static and dynamic behavior of an electropneumatic positioning servomechanism with linear pneumatic actuator and proportional pneumatic distributor, is formed by a system of nonlinear differential equations with five unknowns, respectively the state parameters of the modeled system. The nonlinearity of the mathematical model is given by all the nonlinearities specific to a system in which the physical processes are governed by the equations of flow through holes, adiabatic thermal process equations, equations of mechanical motion in which frictional forces are present, continuity equations in which the compressibility of the fluid thing cannot be neglected.

Even in the working assumptions formulated in the mathematical model description, the mentioned nonlinearities were found in the model description.

5.2 Presentation of numerical simulation languages used in the design of automatic electropneumatic systems

Types of numerical simulation languages used in the design of automatic electropneumatic systems are:

- Simulink-Matlab
- Simcenter Amesim
- VisSim
- Dymola
- Easy5
- 20-sim

5.3. Work methodology in Simcenter Amesim

Of the numerical modeling and simulation programs listed above, Matlab-Simulink and Simcenter Amesim programming environment are widely used in industrial applications for the analysis and synthesis of electric/hydraulic/pneumatic automatic drive systems.
Simcenter Amesim was used for the numerical simulation analysis of the dynamic behavior of the linear positioning electropneumatic servomechanism. The Amesim simulation environment has a friendly and generous graphical interface, including a library of simulation domains such as aeronautics and space; air conditioning; hydraulic components; pneumatic components, etc.

In the HELP section of Simcenter Amesim we can find certain examples and solutions for the different domains, which can help to better understand the software, but also certain solutions to different problems.

5.4. Numerical simulation of the dynamic behavior of linear pneumatic actuators

In pneumatic actuation systems, pneumatic actuators are execution elements that can work both in open loop as pneumatic control units [15, 110], and in closed loop, in command-control-adjustment systems such as positioning systems or tracking [1,15,56,89,110].

This subchapter compares the dynamic behavior of an open-loop linear pneumatic actuator with that of a closed-loop actuator as a positioning system.

The numerical model and numerical simulations were performed with the Simcenter Amesim simulation environment.

Working scenarios for the open loop pneumatic actuator **Table 5.1**

Nr. Crt.	Scenario Name	Distributor Type	Input Signal	Graphical Representations
1	PA-CC-PV-SIMW	DPP closed-center	Sine	Figure 5.8
2	PA-CC-PV-SQRW	DPP closed-center	Square	Figure 5.9
3	PA-CC-PV-TRAP	DPP closed-center	Trapezoidal	Figure 5.10
4	PA-ABT-PV-SIMW	DPP semi-opened ABT	Sine	Figure 5.11
5	PA-ABT-PV-SQRW	DPP semi-opened ABT	Square	Figure 5.12
6	PA-ABT-PV-TRAP	DPP semi-opened ABT	Trapezoidal	Figure 5.13

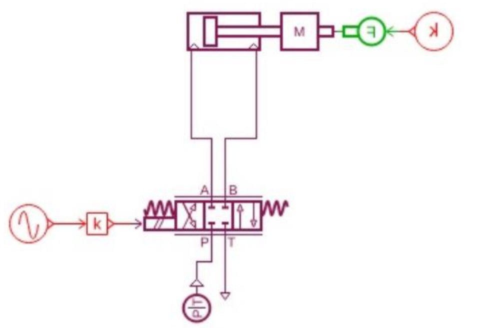

a)

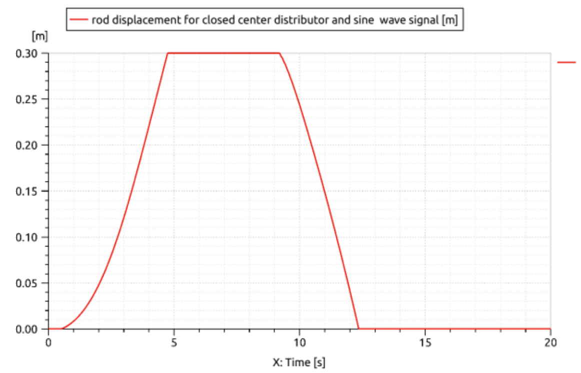

b)

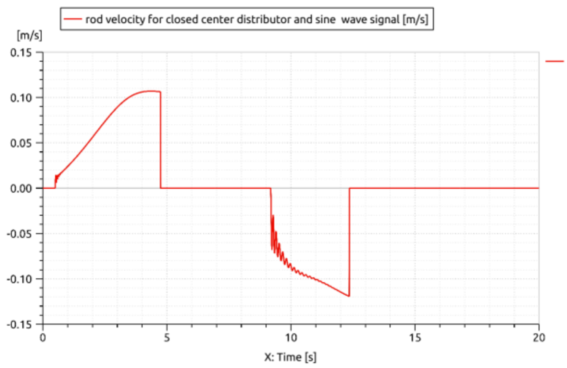

c)

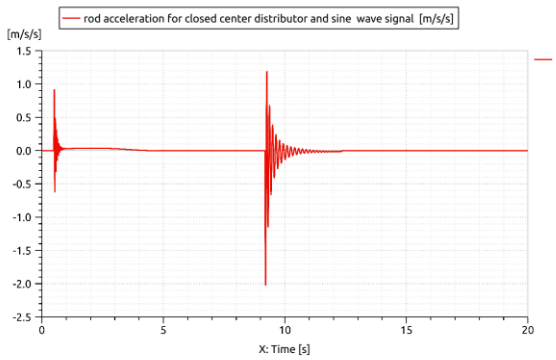

d)

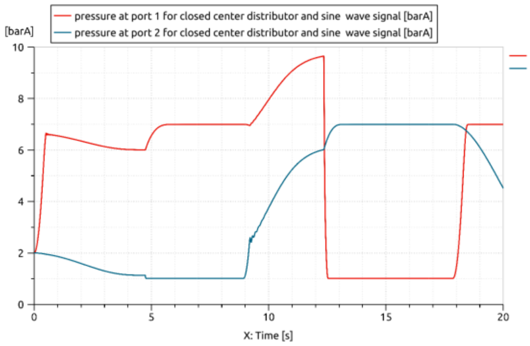

e)

Figure 5.1. PA-CC-PV-SIMW: a) numerical simulation scheme; b) piston displacement variation; c) speed variation; d) acceleration variation; e) pressure variation in the actuator chambers [16]

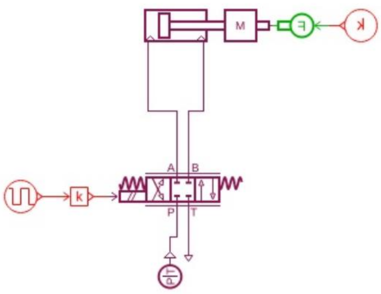

a)

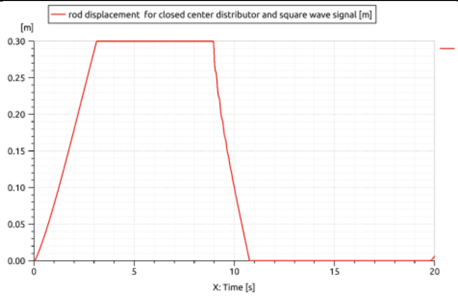

b)

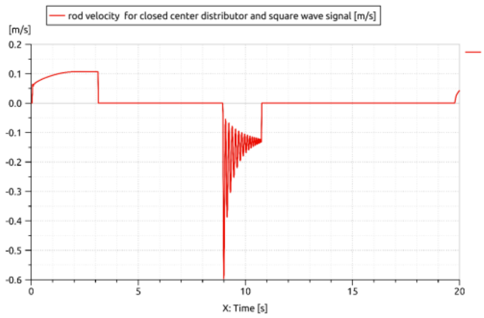

c)

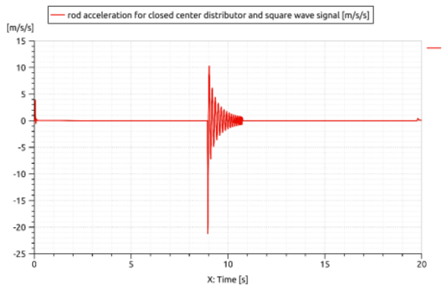

d)

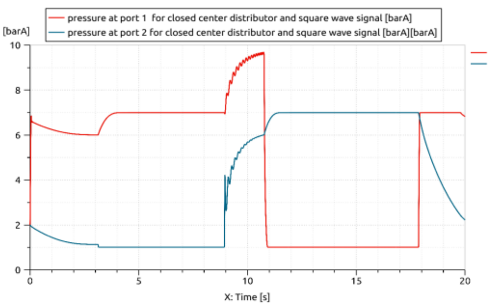

e)

Figure 5.2. PA-CC-PV-SQRW: a) numerical simulation scheme; b) piston displacement variation; c) speed variation; d) acceleration variation; e) pressure variation in the actuator chambers [16]

Theoretically, through the numerical simulations made, it was shown that using a proportional pneumatic distributor the actuation system simplifies the actuation scheme of the pneumatic actuator directly controlled by an on-off pneumatic distributor. Moreover, the dynamics of the open-loop pneumatic cylinder can be easily controlled by changing the electrical input signal of the proportional distributor.

Dynamic behavior of linear pneumatic actuator operating in closed loop

Compared to the numerical simulations regarding the dynamic behavior of the open-loop linear pneumatic actuator, Figure 5.3 shows the structural diagram and the numerical simulation diagram of the closed-loop actuator. The diagram shown is that of an electropneumatic linear positioning servomechanism where the flow amplifier is a proportional pneumatic distributor.

The pneumatic elements in the numerical simulation scheme are the same as previously presented, with the observation that the proportional pneumatic distributor is only with critical center, considering that the dynamic performance of the linear actuator is better than if the DPP is with semi-open center ABT (as seen in numerical simulations).

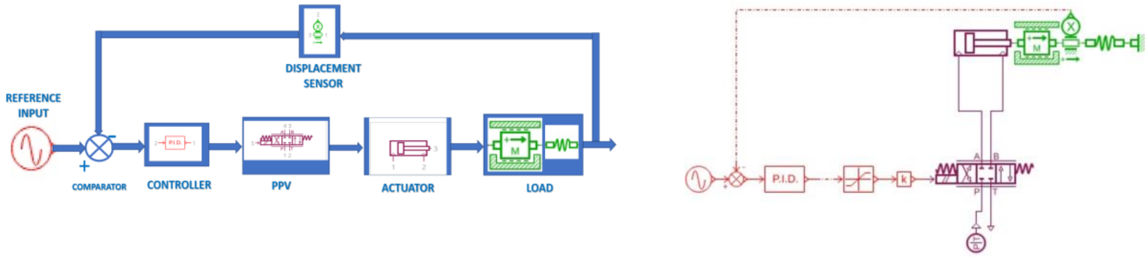

a) b)

Figure 5.3. Block diagram (a) and diagram for numerical simulation (b) of the pneumatic system [22].

In the numerical simulations, the pneumatic actuator has a piston diameter of 100 mm and a rod diameter of 50 mm, and the actuator stroke is 400 mm. In the mathematical modeling of the actuator, a viscous friction coefficient of 75 N s/m and a heat exchange coefficient of 50 $J/m^2/K/s$ were considered, for an external temperature of 293.15 K. In the case of DPP with center- critically, an area of 7 mm^2 and a flow coefficient of 0.72 were considered for the distributor's command and control ports. The natural frequency of the proportional distributor is 80 Hz, and the control current is 10 V. The construction parameters for the pneumatic equipment comply with the FESTO catalog data. The functional parameters, those considering the thermo-hydraulic phenomena in the operation of the equipment, were considered as default data, in accordance with the information from the Simcenter Amesim program library "Lab Pneumatics" [105].

The pneumatic servomechanism must linearly position an inertial load of 25 kg, also considering a variable disturbing technological force, consisting of a constant component of 2000 N and a variable elastic component having an elastic constant of 1000 N/m. the displacement transducer has a constant of 25 V/m. The pressure of the compressed air supplied in the system is 7 barA.

Also, the same working methodology is kept, namely the application of different types of reference signals at the input to the system. The reference input signals are represented in figure 5.15, and have an amplitude of 10 V for all signals and a frequency of 0.05 Hz for the sinusoidal signal and the triangular signal [22]. The trapezoidal signal has the same characteristics as that used in the actuator working in open loop.

a. Static characteristic

Figure 5.4 shows the static characteristic, respectively the hysteresis characteristic for the electropneumatic positioning servomechanism (SEPP) consisting of a linear actuator with an asymmetric piston and proportional pneumatic distributor, Fig. 5.3. The static characteristic was represented from the numerical simulations, for a triangular reference signal with frequency of 0.05 Hz and amplitude of 0.1V, 1V and 10V. The representation of the static characteristic has the amplitude of the reference on the abscissa and the displacement of the actuator rod on the ordinate at different moments of time.

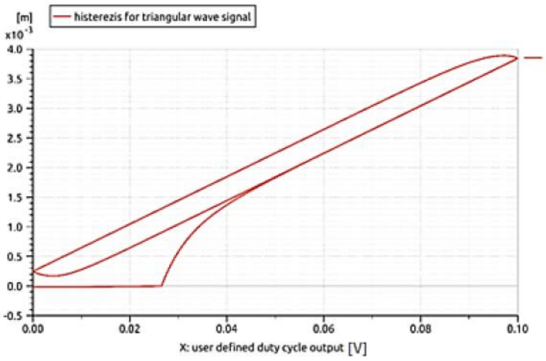

a)

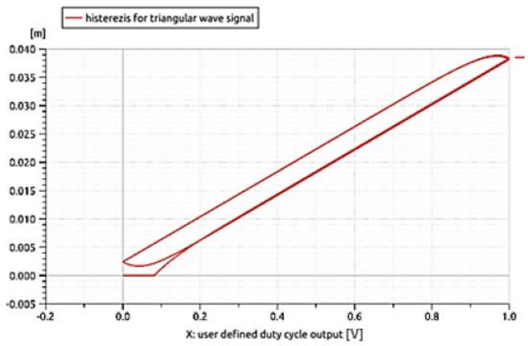

b)

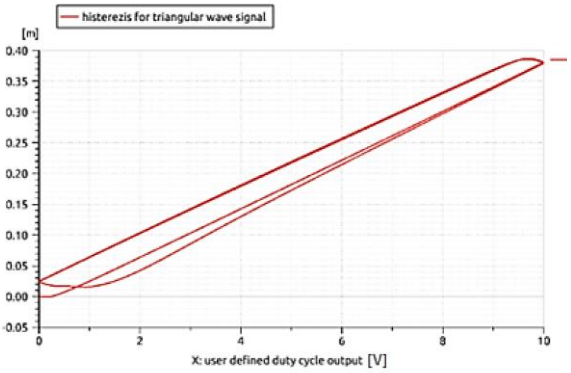

c)

Figure 5.4. Static hysteresis characteristic of SEPP for a triangular signal with an amplitude of 0.1 V (a), 1.0 V (b) and 10 V (c) and with a signal frequency of 0.05Hz [22]

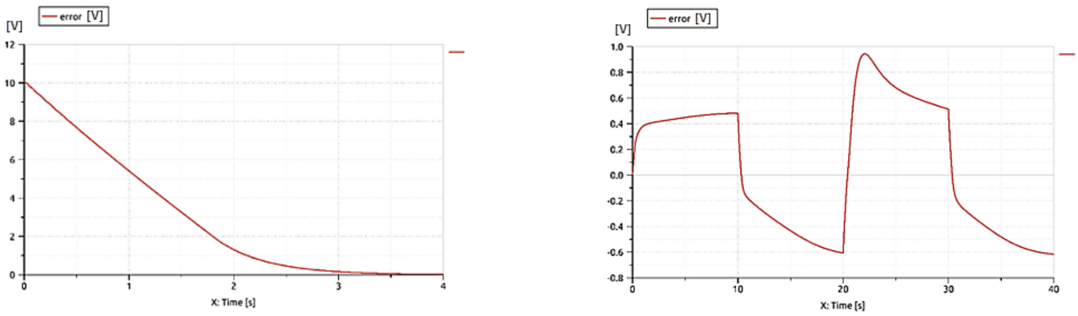

Figure 5.5. SEPP error for different types of reference signals: b) 10 V step input signal, c) 1mA delta input signal [22]

b. Dynamic characteristic

For a sinusoidal reference signal with an amplitude of 10 V and a signal frequency of 0.05 Hz, plot the Bode plot, Figure 5.6. Frequency graph analysis is the response of the system to a sinusoidal input. The sine wave input has an amplitude of 10 V, frequency of 0.05Hz and Bode pattern. A cutoff frequency of 0.2Hz at -3dB and a servo characteristic frequency range of 0.01Hz at 1.5Hz are noted.

In Figure 5.6.b is represented the displacement of the piston having the triangular input signal with the amplitude of 10 V. From the graphic representation it can be seen that the piston follows the input signal and the stroke of the piston has an error of 0.01 mm.

In figure 5.6.c for a trapezoidal input signal the positioning error is zero. In both cases, a small delay is observed at the start of a new cycle, respectively 20 s for the triangular input and 8.15 s for the trapezoidal input [22].

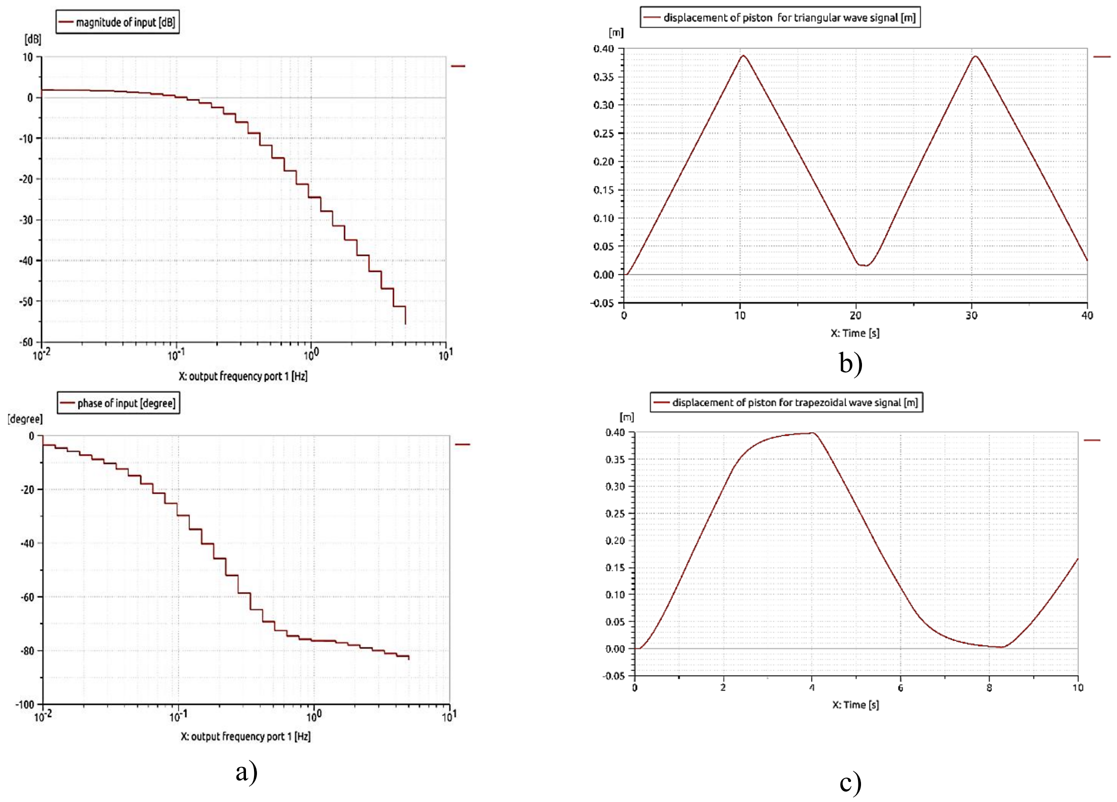

Figure 5.6. Dynamic characteristic of SEPP: a) Bode diagram; b) displacement of the actuator piston to the triangular reference signal; c) displacement of the actuator piston to the trapezoidal reference signal.

c. Dynamic behavior

From the numerical simulations made for different reference signals, the stable behavior of the electropneumatic linear positioning servomechanism was observed. Observations were also made regarding the behavior of the system at a reference step signal, Figure 5.7.

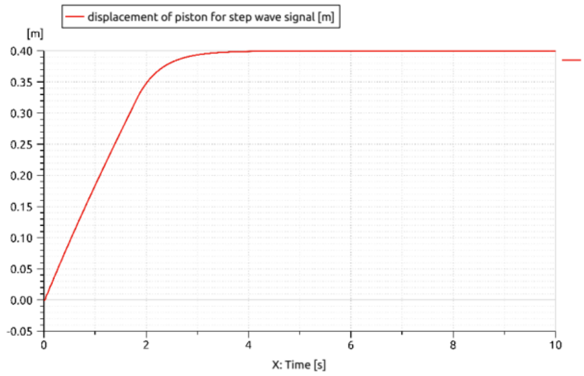

Figure 5.7. SEPP response to step reference signal with 10 V amplitude [22]

At the gear signal, the SEPP servomechanism responds as an over-damped control system, respectively as a first-order control system. On the graphical representation in Figure 5.19 we can read a response time of T=1.397 s, the rise time $T_r = 2{,}13$ and the settling time $T_s = 4{,}08$ s. The response time represents 63.2% of the system response in the case of the step signal and describes the speed with which the control system responds to the reference input. The rise time is 90% of the system response and the settling time is 100% of the system response. The positioning error is zero.

Figure 5.8 shows the dynamic behavior of the SEPP at a sinusoidal reference signal.

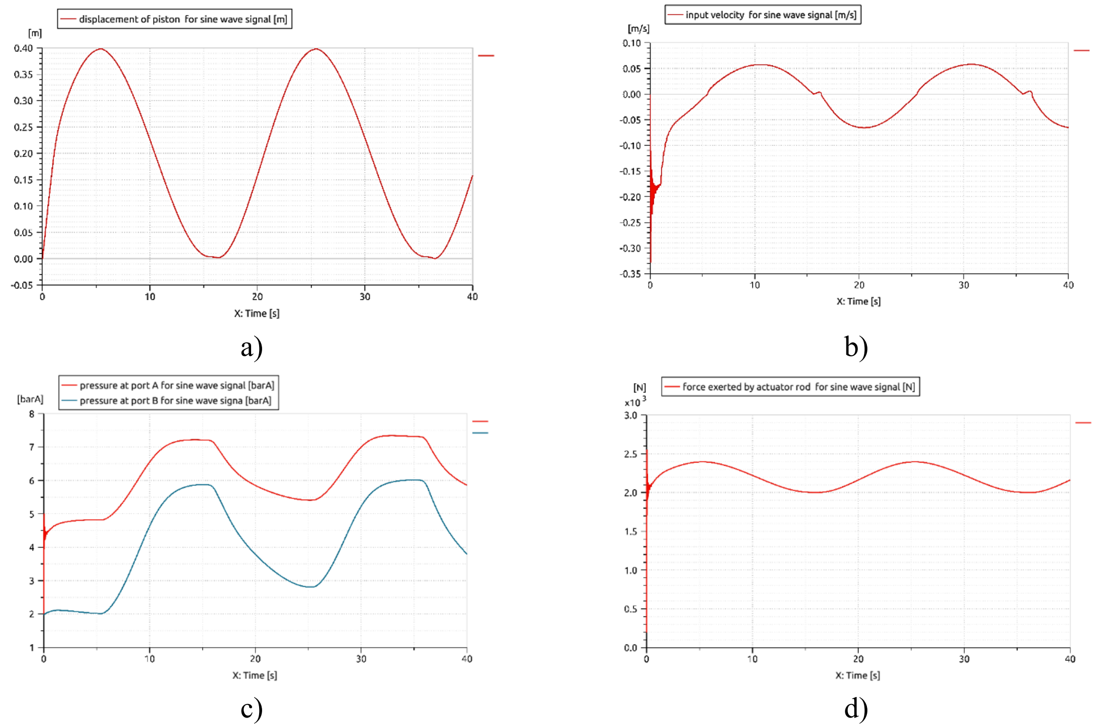

Figure 5.8. SEPP response to sinusoidal input signal with an amplitude of 10 V and a frequency of 50 Hz: a) displacement of the piston, b) speed of displacement, c) pressure in the cylinder chambers, d) force on the piston rod [22]

d. The influence of the coefficient K_p on the dynamics of the system

It was followed how the proportionality constant K_p of the PID regulator influences the dynamic behavior of the servomechanism. For this, the Ziegler-Nichols adjustment method is simplified for proportional control. Thus, for a given step-type signal, different values of the proportionality coefficient K_p were given until the stability of the system is compromised or the system reaches periodic oscillations.

Dynamic performances of SEPP for different values of K_p **Table 5.2**

K_p (-)	Input step 0.1 V				Input step 1 V				Input step 10 V			
	***T* (s)**	**T_d (s)**	**T_r (s)**	**T_s (s)**	***T* (s)**	**T_d (s)**	**T_r (s)**	**T_s (s)**	***T* (s)**	**T_d (s)**	**T_r (s)**	T_s (s)
2	1,979	0,86	3,342	6,81	1,083	0,08	2,431	6,5	1,397	0,02	3	6,8
4	0,974	0,4	1,734	3,3	0,534	0,04	1,215	3,5	1,397	0,02	2,21	4,11
5	0,769	0,31	1,388	3,19	0,436	0,03	0,982	3,02	1,397	0,02	2,13	4,08
6	0,631	0,26	1,156	2,91	0,366	0,03	0,816	2,49	1,397	0,02	2,08	3,38
8	0,471	0,19	0,859	3,5	0,258	0,02	0,594	2,03	1,397	0,02	2,04	3,02
10	0,375	0,15	0,722	2,51	0,226	0,02	0,508	2,51	1,397	0,02	2,04	2,74
12	0,316	0,12	0,535	3,5	0,18	0,02	0,428	3,51	1,397	0,02	2,04	2,58

Table 5.2 shows the values of the delay time T_d, the rise time and the settling time, for different values of K_p, when the input signal is stepped and the amplitude has values of 0.1 V,

1 V and 10 V. It is observed that for a step input of 1 V the system has a time delay with low values even for *Kp*=5.

Also, the quality of the parameters of the pneumatic control system are compromised for K_p> 6, although the oscillation frequency is lower.

Conclusions on the dynamic behavior of the closed-loop DPP-controlled actuator

The dynamic behavior of the linear actuator controlled by a proportional pneumatic distributor was studied through numerical simulations if their operation is in a closed loop. That is, the dynamic behavior of the electropneumatic linear positioning servomechanism was considered. In the structure of the servomechanism, the same pneumatic elements were kept, as in the open loop study.

The static and dynamic characteristic of the SEPP was determined from the numerical simulations. The stable behavior of the positioning system was observed for different reference signals applied and with variable external load applied to the actuator.

Numerical simulations show that positioning accuracy and SEPP dynamics depend on the type of reference signal, reference parameter values, controller parameters, and actuator and pneumatic amplifier characteristics.

Also, values of the proportionality coefficient K_p were found for which the control system remains stable and accurate for the values of the step signal applied as a reference. Numerical simulations show that the system can be adapted to external disturbances by changing the reference signal and the proportional coefficient K_p.

These simulations, together with those of the open-loop pneumatic positioning system, emphasized (at least theoretically) that proportional pneumatic distributor (DPP) pneumatic linear positioning systems are easy to control and represent an alternative to pneumatic servo valve positioning systems .

5.5. Dynamic behavior of electropneumatic positioning servomechanisms with symmetric and asymmetric actuators

In order to study the dynamic behavior of electropneumatic servomechanisms of linear positioning and proportional distributor, the scheme of the pneumatic actuator from the structure of the servomechanism was considered in two constructive variants: actuator with equal piston areas (symmetric actuator) and actuator with unequal equal piston areas (asymmetric actuator).

Using the working facilities offered by the Simcenter Amesim numerical simulation program, the dynamic behavior of the servomechanism considered in the two constructive variants was studied, with the numerical simulation scheme in Figure 5.9. The elements of the numerical simulation scheme have the following meaning and characteristics:

- ✓ Block 1, pneumatic cylinder with symmetrical piston areas (Figure 5.9.a) respectively pneumatic cylinder with asymmetrical piston areas (Figure 5.9.b) stroke of 400 mm, piston diameter of 80 mm and a rod diameter of 25 mm. The area of the symmetrical piston is 4535.67 mm^2. The area of the asymmetric piston is 5026.55 mm2 (large actuator chamber), and 4535.67 mm^2. The air temperature at the inlet is the same as the outlet 293.15 K. The mass displaced by the piston is 30 kg. Coulomb friction force is not considered and the coefficient of viscous friction is 100 N/(m/s). There is no air loss.
- ✓ Block 2, linear displacement transducer with an amplification coefficient of 25 V/m.

- ✓ Block 3 models the disturbance force considered; is an elastic force with an elastic constant of 5000 N/m.
- ✓ Block 4 is modeled the control signal, respectively the reference; the signal used being step.
- ✓ Block 5 is a summation block that compares the reference signal with the displacement signal measured by the transducer.
- ✓ Block 6 models the PID regulator that has the proportional component (amplification) K_p= 1 and without having the derivative and integral components set.
- ✓ Block 7 is a filter with a minimum allowed value of -10V and a maximum value of 10V; thus the electrical control range of the proportional pneumatic distributor is limited to values [-10, 10] V, recommended by the manufacturer [18].
- ✓ Block 8 is a –1 amplifier to change the sign of the proportional distributor control signal.
- ✓ Block 9 represents the proportional pneumatic distributor which is a closed center 4/3 distributor, similar to the closed center 5/3 proportional pneumatic distributor [18]. The distributor frequency is considered at 70 Hz and a damping factor of 0.8. The distributor control hole is 7mm^2 and is the same for all 4 ports. The flow coefficient of the distributor is 0.72.
- ✓ Block 10 models the pneumatic pressure source providing a pressure of 7 barA at a temperature of 293.15 K.
- ✓ Block 11 defines the air properties. Air is assumed to be a perfect gas with a density of 1.18 kg/m3 for an operating temperature of 300 K and an absolute pressure of 1.013 barA. The absolute viscosity is 18,552.10^{-6} Pa·s. The thermal conductivity is 0.026156 W/m/K and the specific heat at constant pressure is 1004.815 J/kg/K.

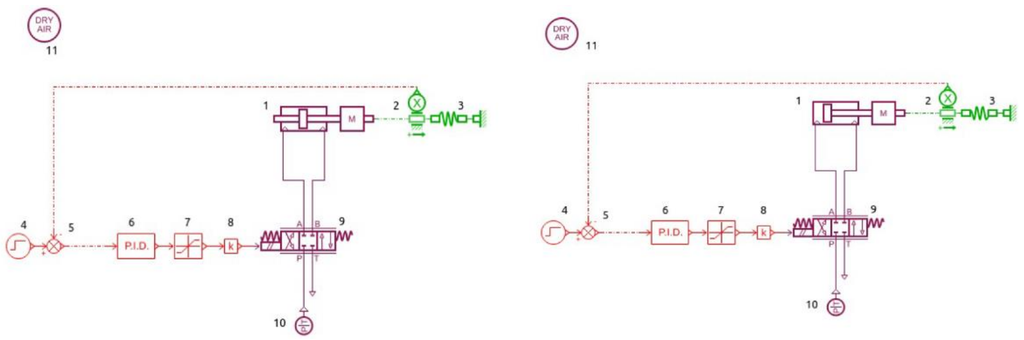

a) b)

Figure 5.9. Actuation scheme with 1- pneumatic cylinder (a) symmetrical and b) asymmetrical); 2- displacement sensor 3- resistive force; ; 4-command signal; 5-adder; 6-PID; 7-block saturation; 8- constant block; 9- proportional distributor 4/3; 10- gas supply source at a pressure of 7barA; 11- type of gas used; 12- constant block [20]

Using the numerical simulation schemes in Figure 5.9, for a step signal of 1 V, the behavior of the electropneumatic servomechanism in the two constructive variants was comparatively analyzed.

As seen in the previous subsection, the studied SEPP electropneumatic servomechanism behaves as a first-order control system, or as an over-damped second-order system. In order to comparatively discuss the behavior of the servomechanisms in the two constructive variants, the quantities defined in Figure 5.10 for a step signal were considered as quantities specific to the dynamic behavior of automatic systems. Let K_T be the time constant of the response $y(t)$, T_r is the rise time and T_s is the settling time. Also, y_{st} is the steady state response of the system.

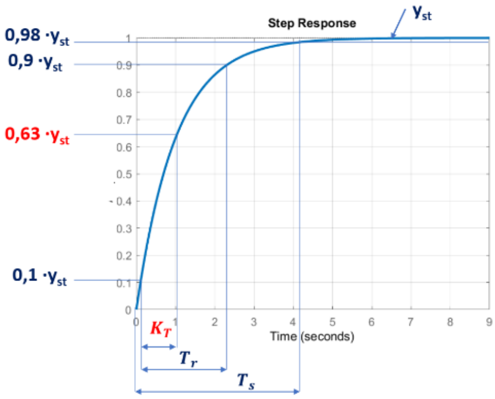

Fig. 5.10. Defining the quantities characteristic of the dynamics of a first-order automatic system

Numerical simulation results for a 1 V step signal are shown in Figures 5.11 and 5.12 for both cases studied.

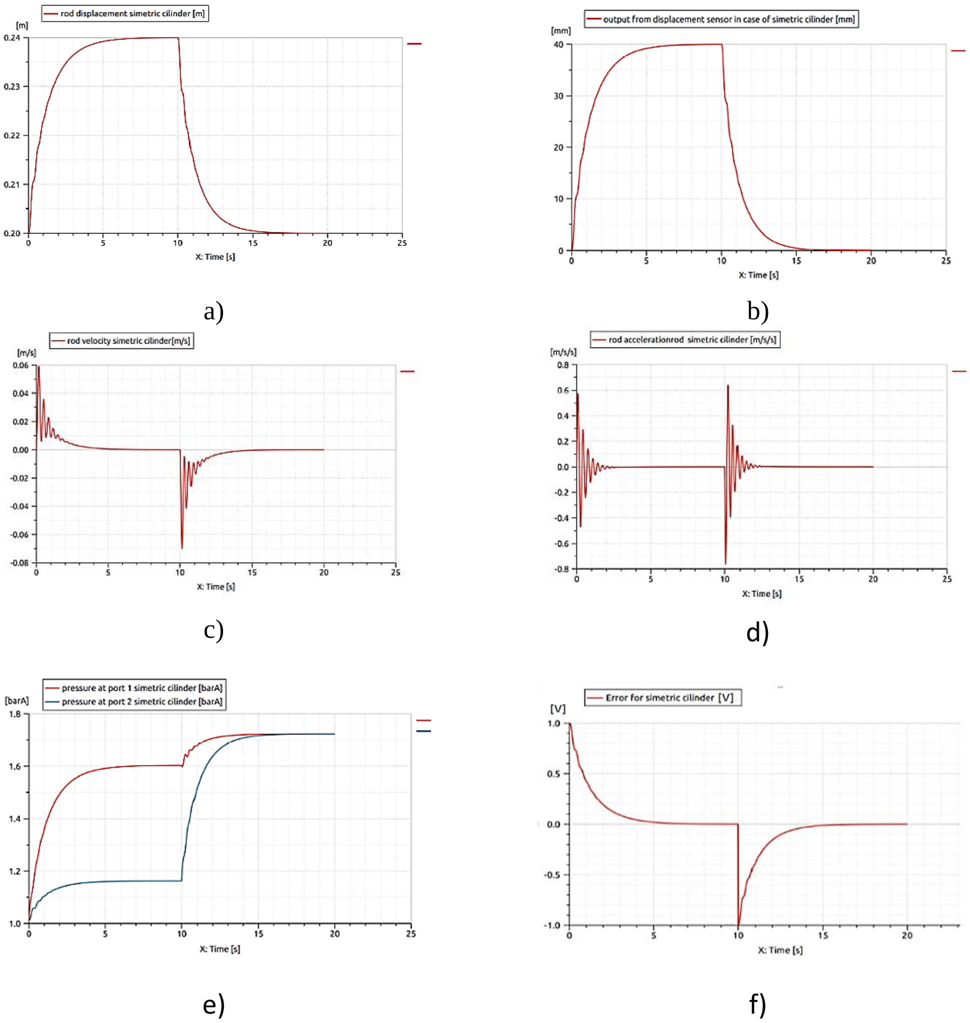

Figure. 5.11. Dynamic behavior of SEPP with symmetrical piston: a) displacement of the rod; b) the output signal of the displacement sensor c) rod speed; d) rod acceleration; e) pressures in the piston chambers; f) positioning error.

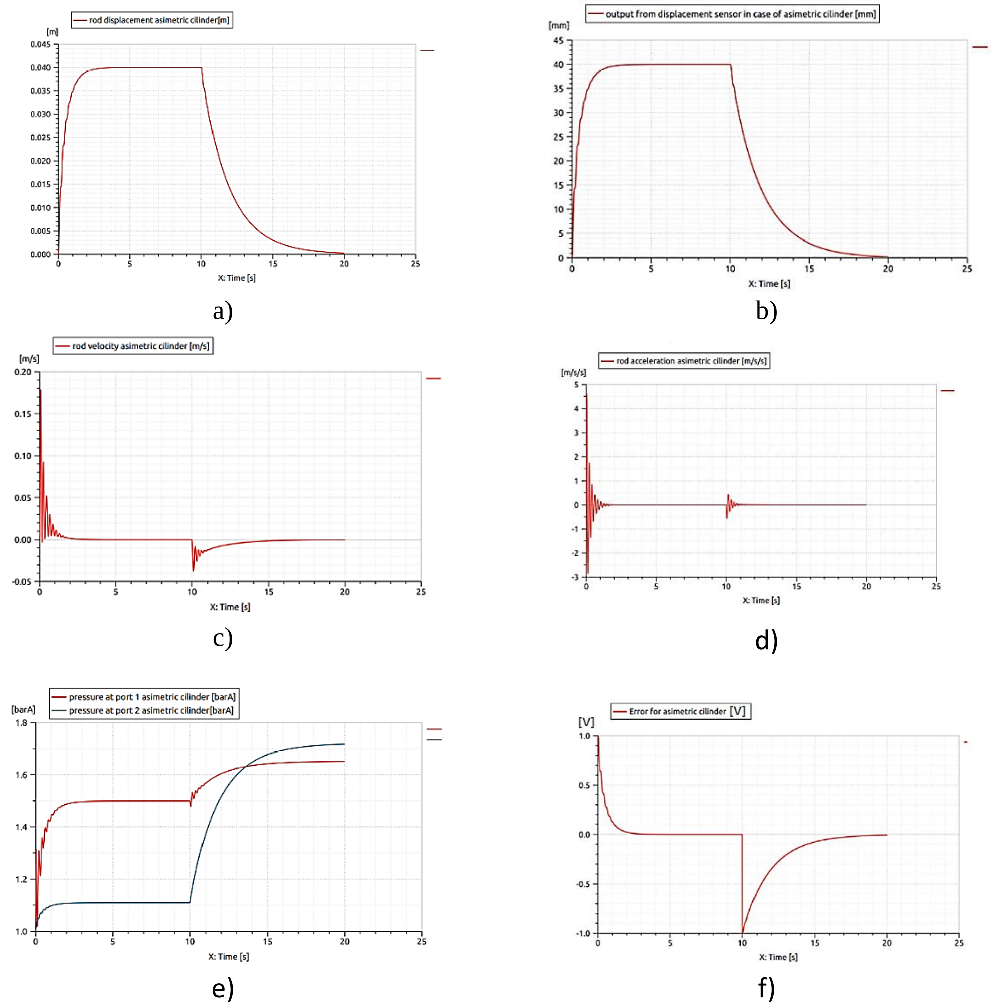

Figure. 5.12. Dynamic behavior of SEPP with asymmetric piston: a) rod displacement; b) the output signal of the displacement sensor c) rod speed; d) rod acceleration; e) pressures in the piston chambers; f) positioning error.

From the above graphs it can be seen that at a 1V step-type control signal, the servomechanism behaves as an over-damped system in both cases studied. To compare the behavior of the two types of servos, the positioning error, rise time and damping time were monitored. The dwell time of the piston when changing the direction of movement by changing the commutation of the proportional pneumatic distributor was also taken into account, Table 5.3.

From Figures 5.11 and 5.12 it is observed that the positioning error is zero for both the symmetric piston servo and the asymmetric piston case.

The two actuators responded to the same type of reference signals considered but the symmetric cylinder starts its movement from the middle of the stroke, while the asymmetric cylinder starts its movement from the end of the stroke.

Dynamic behavior in the case of the step control signal 1 V **Table 5.3**

	Time constant (s)	**Rise time (s)**	**Stabilization time(s)**	**Error (mm)**
The symmetrical cylinder	1.13	2.45	4.8	0
The Asymmetrical cylinder	0.51	1.15	1.92	0

Numerical simulations show that the servomechanisms have stable dynamic behavior and good positioning and tracking performance. The response time of the asymmetric piston is better than that of the symmetric piston, which is why it is recommended for applications that require fast positioning.

5.6. Dynamic behavior of an electropneumatic servomechanism for actuation of a butterfly valve

In a wastewater treatment plant, the technological process of biological treatment is particularly complex with regard to the amount of dissolved oxygen DO introduced into the wastewater to activate biological reactions. The range of dissolved oxygen OD is 1.5 ÷ 2 g/m^3 and must be rigorously controlled [148] . If the DO concentration is too high (> 2 g/m^3) an over-mixing will occur in the biological reactor and a lag in the creation of activated sludge will occur. If the concentration is lower than 1.5 g/m^3, the micro-organisms in the activated sludge will not be able to develop properly to be able to decompose nitrogen and phosphorus compounds [79].

Between 50% and 75% of the energy consumed in a water treatment plant comes from the energy consumption of the oxygen blowers that feed the aeration basins. Under these conditions, an actuation system that reduces air consumption but keeps the OD oxygen level within normal limits is essential to lower electricity consumption. Under these conditions, the operating costs of the treatment plants are also reduced.

In Figure 5.13, it is proposed to operate the butterfly valve with an electropneumatic servomotor that supplies the compressed air supply line to the aerators (porous diffusers) in the wastewater aeration basins.

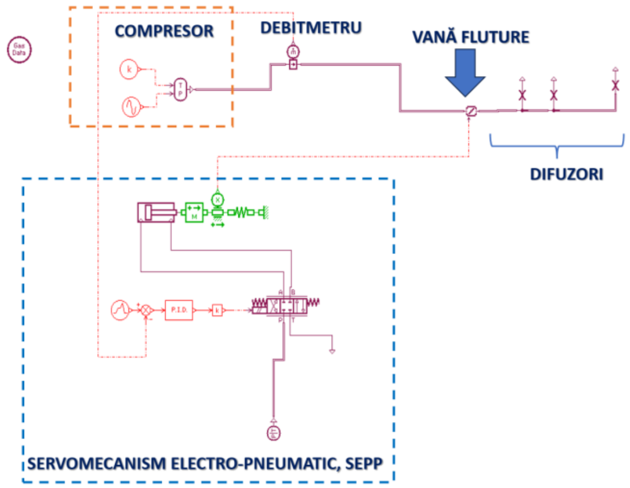

Figure 5.13. Schematic of the SEPP actuation of the butterfly valve in the aeration plant in a water treatment plant

The control of the butterfly valve is done with the help of an electropneumatic SEPP linear positioning servomechanism, similar to the one studied in the thesis. The actuator actuates the lenticular shutter of a butterfly valve with a nominal diameter of 200 mm. Within the automation system, the flow rate is permanently monitored by a flow meter. In the regulation scheme it is observed that the measured flow is compared with the reference signal of the servomechanism which actuates the shutter of the butterfly valve and changes the flow in the installation.

The pneumatic actuator used has a piston diameter of 50 mm, a rod diameter of 12 mm and a stroke length of 0.1 m. In turn, the pneumatic cylinder is controlled by a proportional distributor having the same data as those used in the previous simulations.

The diffusers supplied with compressed air are assimilated with hydraulic resistances and have the surfaces of 325 mm^2, 375 mm^2 and 200 mm$_2$.

The correction of the command signal is done with the help of a PID regulator.

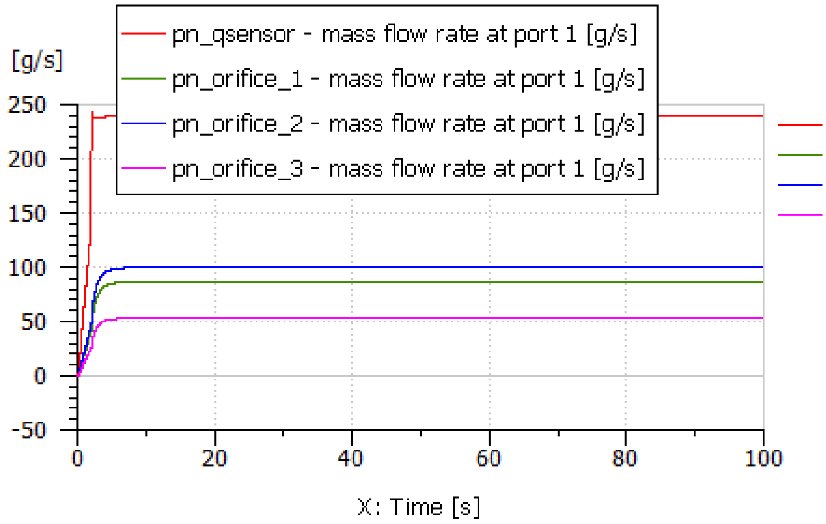

Figure 5.14. The air flow on the compressed air supply line and on each diffuser noted „orifice_1" , „orifice_2" and „orifice_3"

From figure 5.14 it can be seen that the air flow rate is kept constant both on the compressed air supply pipe and on each air diffuser, even in the conditions where the compressor, which supplies the installation, has a sinusoidal variation of the absolute pressure.

From the study made by the method of numerical simulation by means of an evolved simulation language, Simcenter Amesim, it follows that considering the complexity of pneumatic control systems, the use of simple models and modern calculation techniques successfully replace the old prototype testing procedures used in the industry [36].

Nowadays, modern research methods like Model-in-the-Loop (MiL), Software-in-the-loop (SiL) and Hardware-in-the-Loop (HiL) help us shorten the path between conception, design and prototype testing [105].

Chapter VI

EXPERIMENTAL DETERMINATION OF ELECTROPNEUMATIC SERVO-MECHANISM PERFORMANCE

6.1. Overview

In the present chapter, the experimental results for determining the static and dynamic performance of the electropneumatic linear positioning servomechanism are presented. The experimental results were compared with the numerical results considering that the same FESTO pneumatic components as those in the experimental stand were used in the numerical simulation model.

6.2. Structure of the test stand

Figure 6.1 shows the elements of the experimental pneumatic stand. The component elements can be represented in the form of the structural block diagram in Figure 1.1, respectively Fig. 5.3.a. Also, the numerical simulation scheme presented in the previous chapter, Figure 5.3.b, is physically realized with the elements from Fig. 6.1.

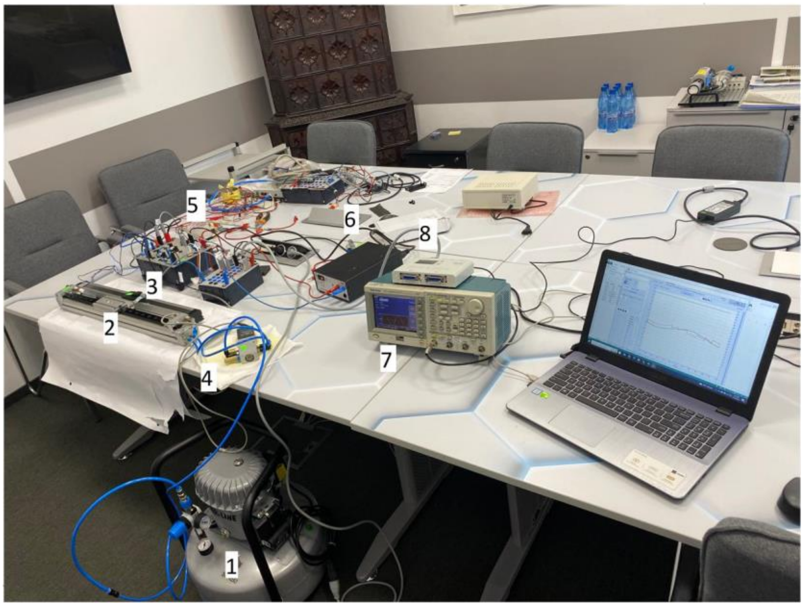

Figure 6.1. Plan view of the experimental stand: 1- air compressor; 2- pneumatic actuator; 3- linear displacement transducer; 4- proportional distributor 5/3; 5- PID regulator; 6-source 24 V; 7- signal generator; 8-data acquisition board [17]

6.3. Work methodology

The pneumatic actuator is supplied with air (absolute pressure 7 barA) from a FESTO compressed air unit. The proportional distributor is controlled by the PID controller powered from a 24 VDC power supply which receives the reference signal from a signal generator. Also, the proportional distributor will control the flow to the pneumatic actuator whose displacement is followed by the displacement transducer.

For data acquisition, a Festo Easy port board was used in the first phase, connected to the USB port of the computer using a USB A-B cable, available in 1.5 meters or 3 meters.

The Easy Port board is also connected to a Festo universal connection unit via an I/O data cable with SysLink connectors, which in turn receives from the PID controller the two analog signals (from the signal generator and from the output from the PID to the proportional distributor), passing them for acquisition to the Easy Port board. An I/O data cable with SysLink connectors is used for data transmission.

The software used to read the data from the acquisition board is FluidLab-M V1, with the acquisition scheme shown in Figure 6.2.

Subsequently, data acquisition was also performed using a Hantek 6022BE oscilloscope and an NI USB-6218 acquisition board to verify the accuracy of the initially recorded data.

In the case of the NI USB-6218 board, the scheme for acquiring the measured values was made using the LabView program figure 6.3, and for the Hantek 6022BE oscilloscope with the help of the Hantek 6022BE V1.0.6 program, Figure 6.4.

Depending on the type of electrical signal transmitted by the signal generator, the electrical signal from the transducer is compared with the reference input from the controller.

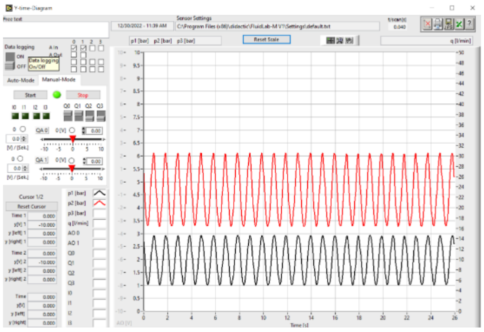

Figure 6.2. Scheme of the acquisition of the measured quantities executed with the aid of the FluidLab-M V1 program

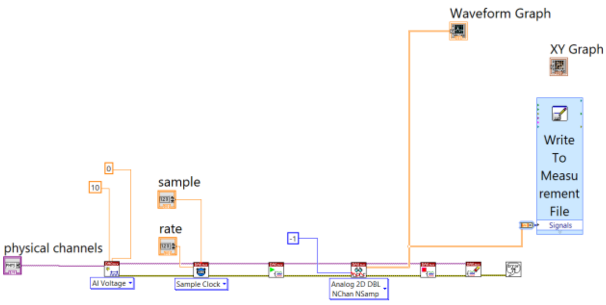

Figure 6.3. The scheme of the acquisition of the measured quantities executed with the help of the LabView program

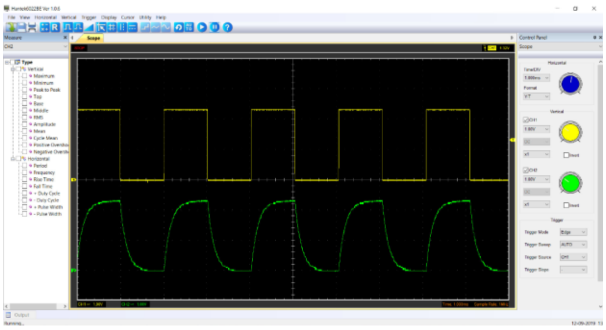

Figure 6.4. Scheme of acquisition of measured quantities executed with the help of the program Hantek 6022BE V1.0.6

Table 6.1 presents the parameters that define the reference signals applied as input quantities in the electropneumatic positioning servomechanism.

Types of reference signals used **Table 6.1**

Signal type	Frequency [Hz]	Amplitude [V]	Offset [V]
Sine	0,1	0,5	2,4
Sine	0,1	1	2,4
Sine	0,5	1	2
Sine	1	1	1
Sine	0,5	1	2,4
Sine	0,5	2	2,4
Sine	0,5	3	2,4
Sine	0,5	4	2,4
Sine	1	1	2,4
Sine	2	1	2,4
Sine	3	1	2,4
Sine	4	1	2,4
Sine	5	1	2,4
Sine	6	1	2,4
Sine	0,1	4	2,8
Sine	1	1	1
Step	0,1	0,5	2,4
Step	0,1	1	2,8
Step	1	1	1
triangular	0,1	0,5	2,4
triangular	0,5	4	2,8

6.4. Experimental results

For the tests performed, reference signals with amplitudes and frequencies consistent with those in Table 6.1 were used.

The static and dynamic characteristics of the SEPP servomechanism were plotted.

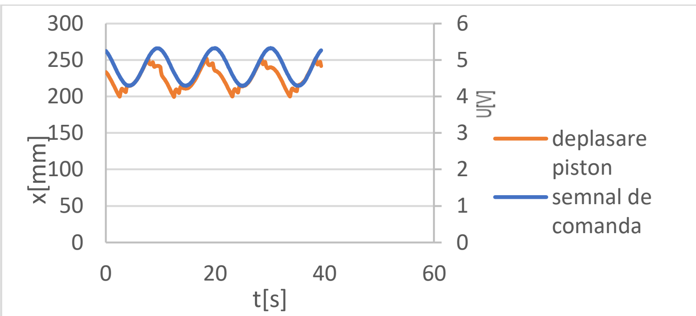

Figure 6.5. Piston displacement for a sinusoidal signal with a frequency of 100 mHz, amplitude 0.5V, Offset 2.4 V, $K_p = 2$

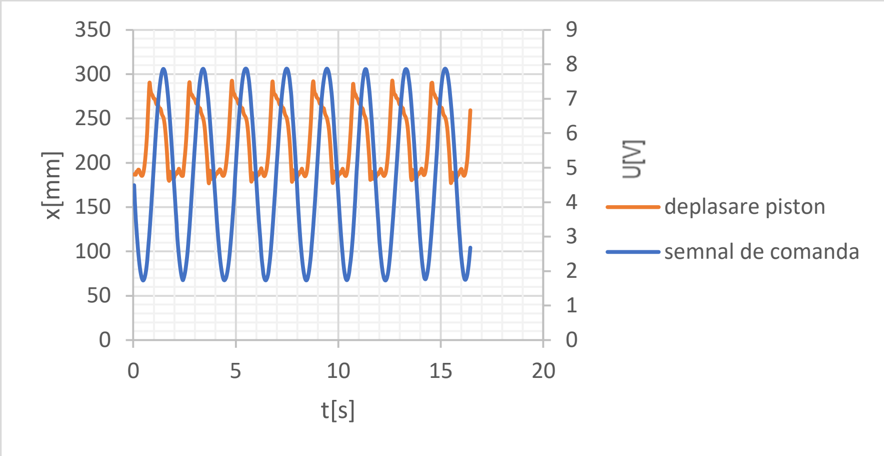

Figure 6.6. Piston displacement in the case of a sinusoidal signal with a frequency of 0.5 Hz, amplitude 3V, Offset 2.4V,K_p=2.

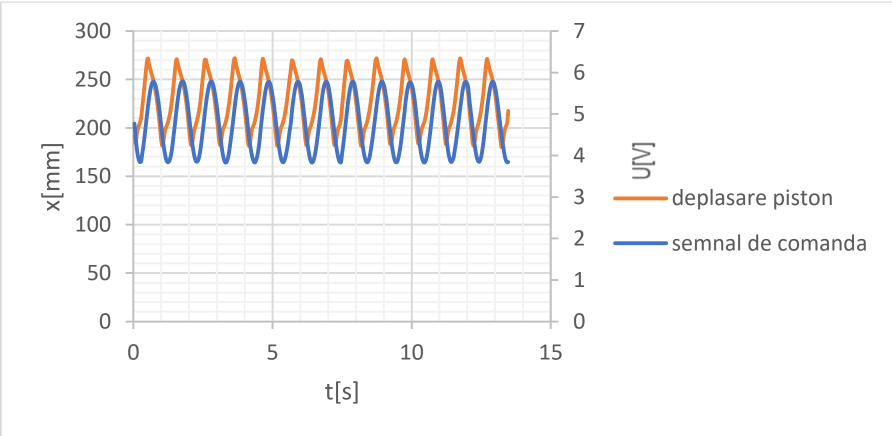

Figure 6.7. Piston displacement in the case of a sinusoidal signal with a frequency of 1 Hz, amplitude 1V, Offset 2.4V, K_p=2.

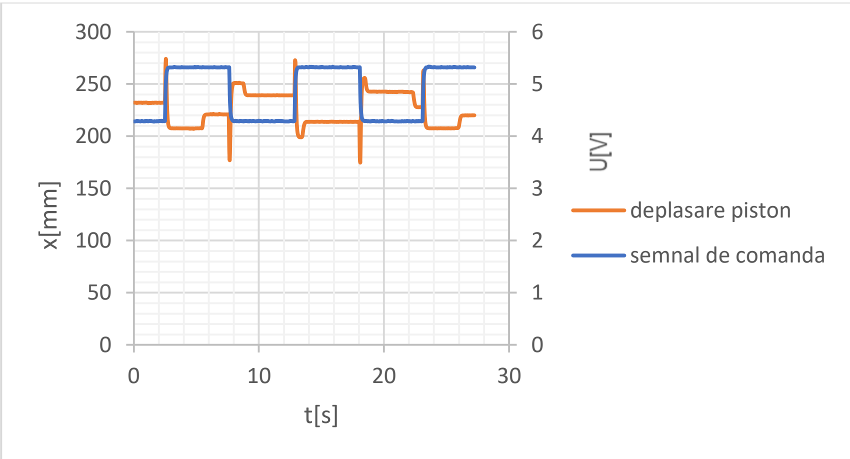

Figure 6.8. Piston displacement for a step signal (rectangular) with a frequency = 0.1Hz, amplitude 0.5V, Offset 2.4V, K_p=2.

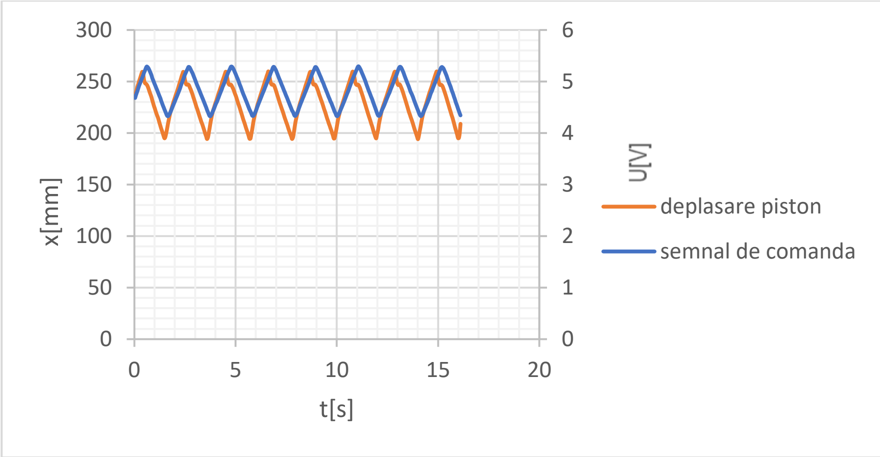

Figure 6.9. Piston displacement in the case of a triangular signal with a frequency of 0.5 Hz, amplitude 0.5V, Offset 2.4V,K_p=2.

Data acquisition was also performed with a Hantek 6022BE oscilloscope with a sampling rate of 1V/s and an acquisition frequency of 100 kHz, with the results shown in Figures 6.10 and 6.11.

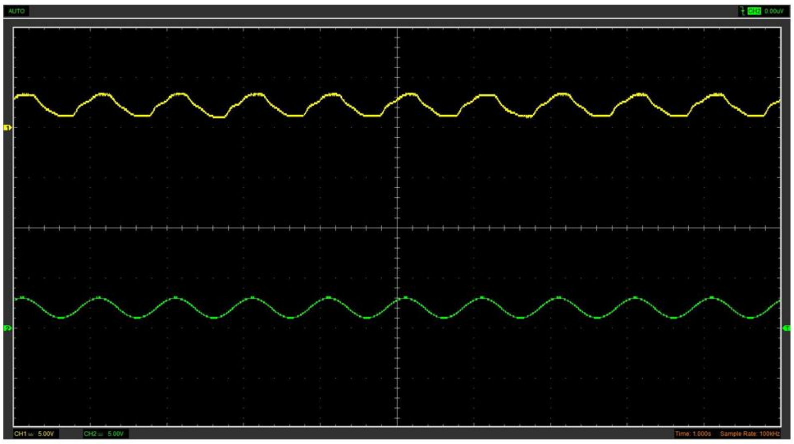

Figure 6.10. Sine volt signal as a function of time with frequency 1Hz, amplitude 1V and Offset 1V. The green line is the command signal, the yellow line is the output signal (Hantek 6022BE oscilloscope)

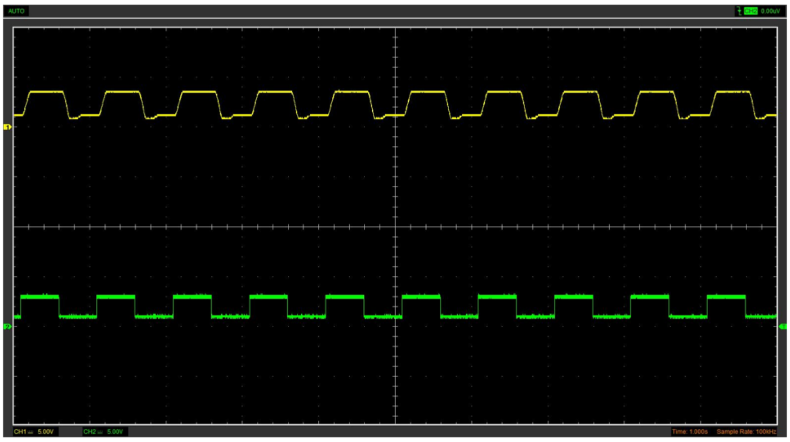

Figure 6.11. Rectangular signal in volts as a function of time with frequency of 1 Hz, amplitude 1V and Offset 1V. The green line is the command signal, the yellow line is the output signal (Hantek 6022BE oscilloscope)

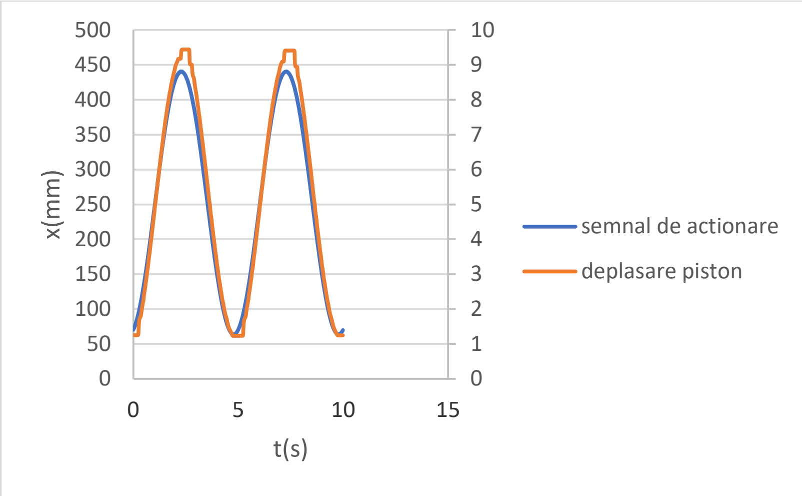

Figure 6.12. Piston displacement in the case of a sinusoidal signal with a frequency of 100 mHz, amplitude 4V, Offset 2.8 VK_p = 4

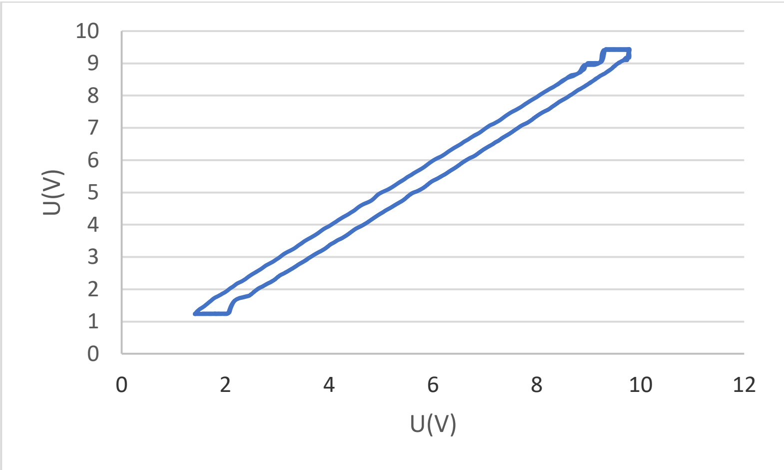

Figure 6.13. Static characteristic of SEPP (hysteresis) in the case of a sinusoidal signal with a frequency of 100mHz, amplitude 4V, Offset 2.8V, K_p = 4

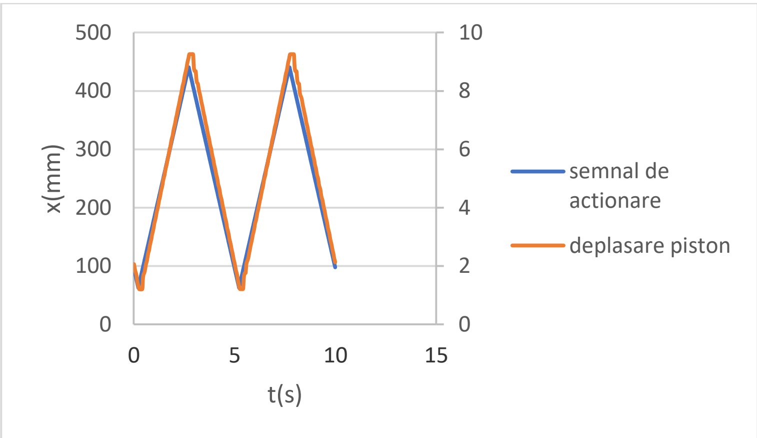

Figure 6.14. Piston displacement for a triangular signal with a frequency of 100 mHz, amplitude 4V, Offset 2.8 V,K_p = 4

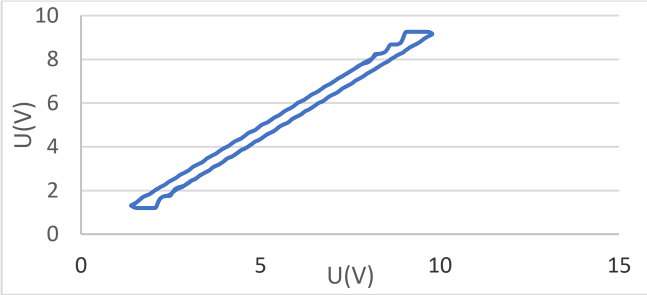

Figure 6.15. Static characteristic of SEPP in the case of a triangular signal with a frequency of 100mHz, amplitude 4V, Offset 2.8V, $K_p = 4$

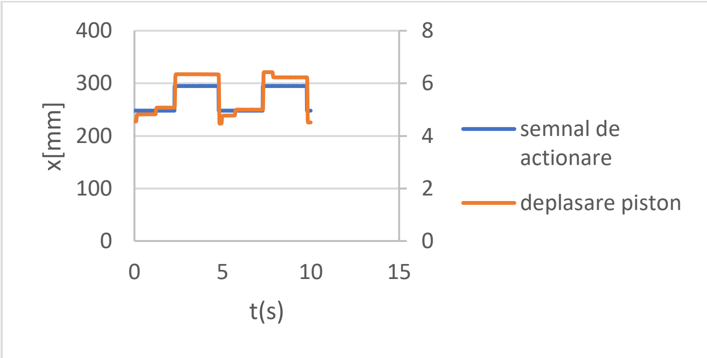

Figure 6.16. Piston displacement in the case of a step signal with a frequency of 100 mHz, amplitude 1V, Offset 2.8 V, $K_p = 2$

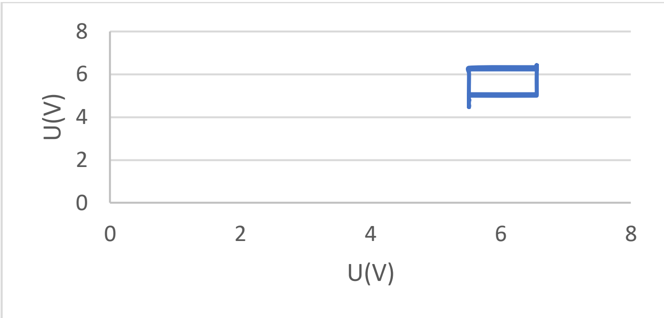

Figure 6.17. Static characteristic of SEPP for a step signal with a frequency of 100 mHz, amplitude 1V, Offset 2.8 V,$K_p = 2$

Figure 6.18 shows the result obtained for a triangular reference signal. As can be seen, the actuator cannot track the input signal.

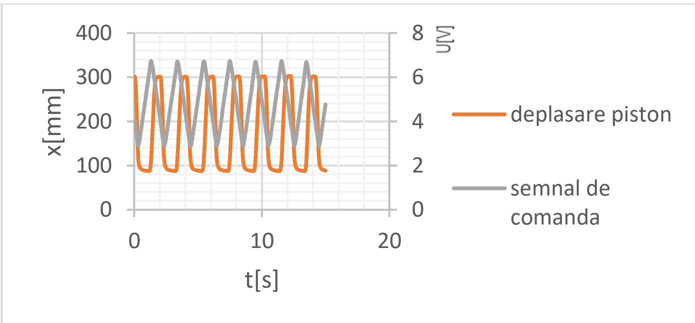

Figure 6.18. Piston displacement for a triangular signal with a frequency of 500 mHz, amplitude 2V, Offset 2.4 V

6.5. Conclusions and comparison with numerical results

Figures 6.5–6.17 graphically represent the reference signal and the response of the electropneumatic servo to these signals. The measurements taken into account both the behavior of the pneumatic actuator in open loop (figures 6.18) and in closed loop.

The experimental data had, throughout the experiments, several types of acquisition plates. The technical characteristics of the acquisition boards used influence the quality of the recorded information.

In the case of data acquired with Festo's Easy Port board, the output is seen to follow the input, but the deadband/resolution of the acquisition board was found to be in the range of 100 ÷ 250 mV, depending on the position of the plunger, with higher values towards the end of the race.

In the case of figures 6.10 and 6.11, due to the very high frequency with which the data acquisition was done, a distortion of the input and output signals is observed. Data acquisition was performed using the Hantek 6022BE oscilloscope.
Considering the results of the numerical simulations presented in the previous chapter, we can say that the results of the numerical simulation are comparable to the experiments, Figure 6.19.

Even the quasi-linear characteristic of the hysteresis curve is approximately replicated. The drop seen in Figure 6.20 is due to the sudden openings of the distributor. As speed is a derivative of displacement, over a short period of time the values are large.

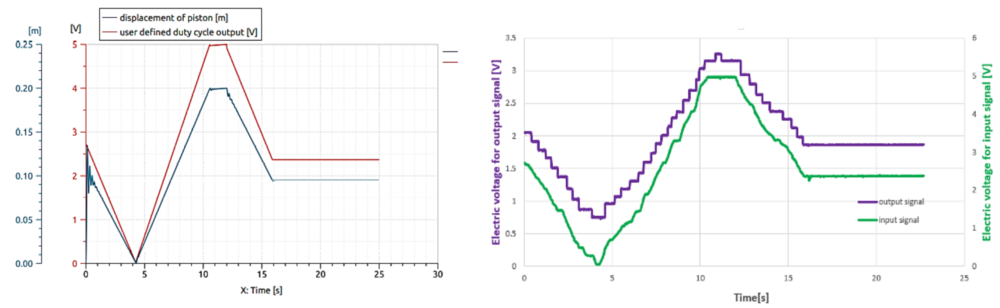

a) b)

Figure 6.19. Simulation results for an input signal a) numerical simulation; b) standing result [23]

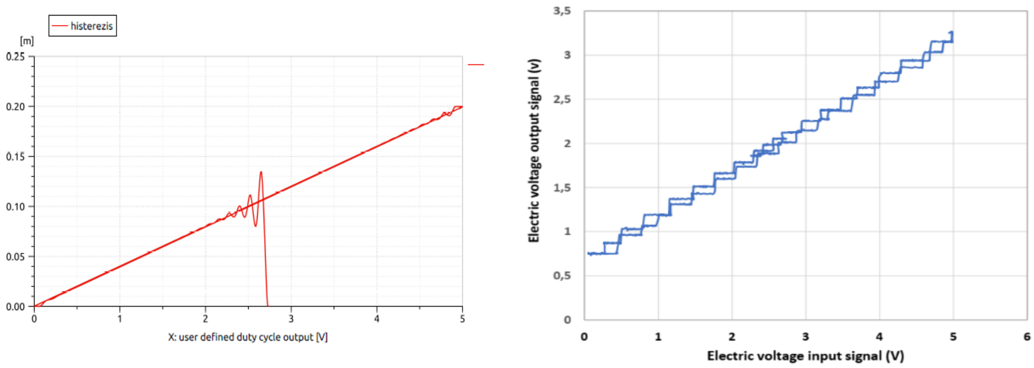

a) b)

Figure 6.20. Hysteresis a) numerical simulation; b) standing result [23]

The experimental results regarding the behavior of the SEPP electropneumatic linear positioning servomechanism at different reference signals, in the conditions where no disturbing force is exerted on the SEPP, show a stable behavior in which the positioning system follows the input signal.

The static (hysteresis) characteristic of the SEPP could also be represented from the experiments.

Table 6.2 shows the experimentally recorded positioning error and delay time.

Poor system resolution can be explained by mechanical friction in the system, or the fact that the controller used was not connected well enough, or because of the acquisition board used (in the case of data acquired with the Hantek data board).

Positioning error and delay time **Table 6.2**

Signal type	Positioning error **(%)**	delay time **(s)**	**Figure nr.**[5]
Sine	3.26	1.55	6.6
Sine	4.65	0.24	6.14
Triangular	2.82	0.25	6.22
Sine	3.6	- 0.45	6.25
Triungular	4.43	- 0.13	6.27
Step	2.29	- 0.34	6.29

Regarding the positioning error of the electropneumatic servomechanism, it is observed that it is less than 5% in all the situations studied, with higher values for the input signal with high frequency or amplitude.

For the open-loop behavior of the pneumatic actuator (obtained by removing the regulator from the actuation loop), it is observed to have uncontrolled motion (in the sense that the actuator piston does not follow the input signal). The actuator piston reciprocates according to the amplitude value of the signal, regardless of its type.

The results obtained in the present work, both through numerical and experimental simulations, emphasize the fact that proportional pneumatic distributors are equipment with special technical qualities that can successfully replace pneumatic servo valves. Moreover, the use of proportional pneumatic distributors is useful in applications regarding the digitization of technological processes considering the possibility of using HART communication protocols in the control of these devices.

Also, the application presented in the paper (paragraph 5.6) regarding the actuation of a future valve for the supply of compressed air to the porous diffusers in the aeration system of the bioreactors in the wastewater treatment plants, can be extended to other pressure pipeline installations. The advantage of using an electropneumatic servomechanism for valve actuation in pipeline systems is given by the optimization of the fluid consumption in the pipelines according to the consumption and thereby the optimization of the energy consumption of the energy generators used in the pipeline system.

[5] As in the Thesis.

Chapter VII

SYNTHESIS OF THE MAIN SCIENTIFIC AND TECHNICAL CONTRIBUTIONS OF THE WORK. FUTURE DIRECTIONS OF RESEARCH

7.1. General conclusions

The main goal of the PhD thesis Proportional electropneumatic servomechanism, SEPP, for the actuation of valves in the energy industry, was to determine the technical possibilities offered by the use of the proportional pneumatic distributor in the structure of a linear positioning electropneumatic servomechanism (called SEPP in the paper) for command and control the actuation of different types of valves used in the energy industry.

As part of the doctoral research, the following theoretical, numerical and experimental studies were carried out:

- Bibliographic study on the performance of electropneumatic servomechanisms that use the proportional pneumatic distributor as a pneumatic amplifier in their structure.
- The study by numerical and experimental simulations of the open-loop dynamic behavior of a pneumatic actuator controlled by a DPP proportional pneumatic distributor.
- The study by numerical simulations of the SEPP behavior with the actuator controlled by a DPP regarding the influence of the disturbing force on the positioning error.
- Conception and construction of an experimental test stand, for carrying out experimental studies related to the performance of the SEPP pneumatic system.
- Identification of the elements of the numerical simulation scheme of SEPP, so that they correspond to the elements of the experimental test stand.
- Numerical simulations to determine the performance of the pneumatic actuation servomechanism with DPP, used for the control and command of a butterfly valve, mounted on the supply pipe of the aerators in a wastewater treatment plant.
- Study of the advantages of digitizing the pneumatic actuation servomechanism with DPP.

Chapter 1 presents a brief introduction to the topic of the paper, after which the author presents the objectives and motivation of this paper. At the end of this chapter, the structure of the thesis by chapters is presented.

Chapter 2 presents a brief history of pneumatics, market trends of pneumatic systems. The current status for different types of pneumatic actuators is presented, as well as different theoretical and experimental studies carried out by other authors.

The description of pneumatic servomechanisms, the component elements for these systems is carried out in **Chapter 3**. Also in this chapter, working fluid properties, flow pressure ranges and flow diameters, examples of closed-loop pneumatic actuation schemes and open, but also experimental research carried out by other authors with modern pneumatic actuation systems.

In **Chapter 4**, theoretical aspects related to the flow of compressible fluid through orifices and nozzles are addressed, the flow-pressure characteristics through the orifices of a pneumatic distributor are analyzed and the equations that constitute the mathematical model of an electropneumatic linear positioning servomechanism are detailed.

Chapter 5 focuses on the results obtained from the numerical simulations, which are the basis of the performance validation of the pneumatic system actuated by a proportional distributor. This chapter includes information about the types of software used for numerical simulations, as well as the methodology used in this process. The results of the numerical simulations are presented for the study of the dynamic behavior of the linear pneumatic actuator controlled by the proportional pneumatic distributor if the pneumatic elements are operated in open loop, respectively in closed loop when the system becomes an electropneumatic servomechanism.

Also in this chapter, a comparative study was made regarding the performances of the electropneumatic linear positioning servomechanism having in its structure a pneumatic actuator with equal piston areas versus an actuator with unequal piston areas.

Chapter 5 concludes with the presentation of the numerical results regarding the use of the electropneumatic positioning servomechanism in actuating the air flow supply valve of the aerators in the biological stage of a sewage treatment plant. It is aimed to maintain a constant flow rate in the system at the pressure variations that occur in the technological process.

Chapter 6 focuses on the experimental validation of the results obtained from the numerical simulations. This chapter contains information about the methodology used in the experimental tests, the results obtained, comparisons between the numerical and experimental results. Finally, the conclusions obtained from these experiments are presented.

7.2. Original contributions

This thesis makes a series of original contributions in terms of both numerical and experimental study of the performances of SEPP electropneumatic linear positioning servomechanism with proportional distributor in its structure.

a) Numerical contributions

- Realization of the theoretical study regarding the flow of compressible fluid through holes and nozzles, with the determination of the flow-pressure characteristic through the holes of the pneumatic distributor Fig. 4.3, Fig. 4.6, Fig. 4.7, Fig. 4.8.
- Realization of numerical simulations regarding the dynamic behavior of proportional distributors figures 4.11÷4.20.
- Validation, by comparing the results of the numerical simulations with those existing in the specialized literature, Figure 4.21.
- The presentation, from the bibliographic study done, regarding the influence of non-linearities on the performance of electropneumatic positioning servomechanisms and the types of regulators used to compensate for non-linearities.
- Determining the equations that define the mathematical model of an electropneumatic linear positioning servomechanism.
- Carrying out numerical simulations to determine the dynamic behavior of the open-loop linear pneumatic actuator for different reference signals, Figures 5.8 to 5.13.
- The study of the dynamic behavior of the electropneumatic linear positioning servomechanism at different reference signals with the tracing: static characteristics Figure 5.16; dynamic characteristics Figure 5.18; dynamic behavior Figure 5.19; the

influence of the proportionality coefficient of the regulator K_p on the dynamics of the system, Figures 5.21 and 5.22.

- The comparative study regarding the dynamic behavior of electropneumatic linear positioning servomechanisms using actuators with equal areas in their structure compared to the case of using actuators with unequal areas, Fig. 5.25 to Fig. 5.29.
- The study on the dynamic behavior of an electropneumatic servomechanism for the actuation of a future valve, Fig. 5.30 to Fig. 5.35.

b) Experimental contributions

- Realization of the experimental stand for the study of the dynamic behavior of the electro-pneumatic positioning servomechanism, Figure 6.1.
- Experimental measurements to determine the dynamic performances, for different types of control signals (sinusoidal, trapezoidal, triangular, step), figures 6.6 – 6.30.
- Experimental calibration of numerical simulation model parameters.
- Validation, by comparing the results of the numerical simulations with those existing in the specialized literature (fig. 4.26).
- Comparison of numerical and experimental results, Figure 6.34 and Figure 6.35

The experimental results regarding the behavior of the SEPP electropneumatic linear positioning servomechanism at different reference signals, in the conditions where no disturbing force is exerted on the SEPP, show a stable behavior in which the positioning system follows the input signal.

The static (hysteresis) characteristic of the SEPP could also be represented from the experiments.

Table 6.3 shows the experimentally recorded positioning error and delay time.

7.3. Future research directions

From the knowledge gained in the development of the subject regarding electropneumatic linear positioning servomechanisms that use the DPP proportional pneumatic distributor as an amplifier, based on the theoretical and experimental results obtained, I propose the following future research directions:

- ❖ Comparative study on the static and dynamic performances of electropneumatic servomechanisms with proportional distributor versus positioning systems that use on-off solenoid distributors with PWM control.
- ❖ Optimization of the regulator for the control of the electropneumatic servomechanism in order to reduce the non-linearities given by the phenomenon of friction and air compressibility.
- ❖ The theoretical and experimental study regarding the behavior of the electropneumatic positioning servomechanism with variable load. Coupling of the actuator to a butterfly valve will be considered. The hydrodynamic force on the butterfly valve plug is the variable load applied to the actuator.
- ❖ Analytical study of the equations of the mathematical model that define the behavior of the electropneumatic servomechanism with consideration of the friction force.
- ❖ Analytical study of the equations of the mathematical model that define the behavior of the electropneumatic servomechanism considering the delay time.

Thesis bibliography

[1] H. I. Ali, S. B. B. Mohd Noor, S. M. Bashi, M. H. Marhaban, A Review of Pneumatic Actuators (Modeling and Control), *Australian Journal of Basic and Applied Sciences*, 3(2): 440-454, 2009, ISSN 1991-8178

[2] H. I. Ali, S. B. B Mohd Noor, S.M. Bashi, M. H. Marhaban, Mathematical and Intelligent Modeling of Electropneumatic Servo Actuator Systems, *Australian Journal of Basic and Applied Sciences*, 3(4): 3662-3670, 2009 ISSN 1991-8178

[3] S. Anghel, G. Matache, A.–M. Popescu, I.-C. Gîrleanu, Applications of proportional pneumatic equipment in industry, *Magazine of Hydraulics, Pneumatics, Tribology, Ecology, Sensorics, Mechatronics "HIDRAULICA"* (No. 2/2013) ISSN 1453 – 7303

[4] M. I. P. Azahar, A. Irawan, R. M. T. Raja Ismail, Adjustable Convergence Rate Prescribed Performance with Fractional-Order PID Controller for Servo Pneumatic Actuated Robot Positioning, *Cognitive Robotics 3 (2023) 93–106*, https://doi.org/10.1016/j.cogr.2023.04.004

[5] P. Beater, *Pneumatic Drives. System Design, Modelling and Control*, ed. Springer, 2007, ISBN-10 3-540-69470-6

[6] J. F. Blackburn, G. Reethof, and J. L. Shearer, *Fluid Power Control* (New York: The Technology Press and J. Wiley), 1960.

[7] V. Blagojević, M. Stojiljković, Mathematical and simulink model of the pneumatic system with bridging of the dual action cylinder chambers UDC 621.5:62_522, Faculty of Mechanical Engineering Niš, University of Niš, Aleksandra Medvedeva 14, 18000 Niš, Republic of Serbia, Received September 14, 2007, pag 24-26

[8] M. Blokker, C. Di Cristo, A. Gentile, R. Gargano, K. van Laarhoven, A. Leopardi, C. Quintiliani and I. Vertommen, 2021, Optimal Valve Operation for Restoring Functionality of WDN during Critical Events, *Environ Sci Proc 2020* doi:10.3390/environsciproc2020002032

[9] X. Brun, M. Belgharbi, S. Sesmat, D. Thomasset, S. Scavarda, Control of an electropneumatic actuator: comparison between some linear and non-linear control laws. Proceedings of the Institution of Mechanical Engineers, Part I: *Journal of Systems and Control Engineering, SAGE Publications*, 1999, 213 (5), pp.387-406. ff10.1243/0959651991540232ff. ffhal-00141155ff

[10] C. R. Burrows, Webb, C.R. *Simulation of an On-Off Pneumatic Servomechanism*, Proc. Inst. Mech. Eng. 1967,182, pp 631–642.

[11] C. R. Burrows, Webb, C.R., *Further Study of a Low-Pressure on-off Pneumatic Servomechanism*, Proc. Inst. Mech. Eng. 1969, 184, pp 849–858.

[12] C. R. Burrows, *Fluid power servomechanisms*, Ed. London, New York, Van Nostrand Reinhold Co, 1972

[13] I. Catană, V. Panduru, *Conducerea inteligentă a sistemelor electrohidraulice. Construcție, Modelare, Control*, Ed. Printech, 2004

[14] S. Čajetinac, D. Šešlija,V. Nikolić, M. Todorović, Comparison of pwm control of pneumatic actuator based on energy efficiency, *facta universitatis Ser: Elec. Energ*. Vol. 25, No 2, August 2012, pp. 93 – 101 DOI: 10.2298/FUEE1202093C

[15] G. Chaohui, W. Chenggang, Controller Design for a Pneumatic Actuator System with Proportional Valve, *International Journal of Simulation - Systems, Science & Technology*, 17, Issue 2, p10.1-10.7, DOI 10.5013/IJSSST.a.17.02.10, (2016).

[16] V. N. Cococi, C.-A. Safta, and C. Călinoiu, Dynamic behaviour of proportional pneumatic valves of the actuators in open-loop, *E3S Web of Conferences* 180, 04012 (2020) *TE-RE-RD 2020*, https://doi.org/10.1051/e3sconf/202018004012

[17] V. N. Cococi, C. Calinoiu, Al. Marin si C. A. Safta, Water Valves in Water Digitalization Process. Numerical and Experimental Approach, *Journal of Hydroinformatics*, Special Issue: HIC 2022

[18] V. N. Cococi, C. Calinoiu, Al. Marin* and C. A. Safta, Water Valves in Water Digitalization Process. Numerical and Experimental Approach, *Journal of Hydroinformatics* 2023

[19] V. N. Cococi, C.-A.Safta, C. Călinoiu, Dynamic behaviour of pneumatic actuators in open-loop controlled by proportional valves, *E3S Web of Conferences 180, 04012 (2020),* https://doi.org/10.1051/e3sconf/202018004012

[20] V. N. Cococi, C. A. Safta, Dynamic behavior of a pneumatic servomechanism with symmetric piston's area cylinder versus an asymmetric ones, Buletin UPB ID 1435

[21] V.N. Cococi, C.-A. Safta, C. Calinoiu, Numerical simulation approach of a pneumatic actuator to force perturbation, *EPE 2020 - Proceedings of the 2020 11th International Conference and Exposition on Electrical And Power Engineering*, 2020, pp. 589–593, (2020) 9305558

[22] V. N. Cococi, C.-A. Safta, C. Călinoiu, Parameter tuning process for a closed-loop pneumatic actuator, *IOP Conference Series. Earth and Environmental Science; Bristol Vol. 664, Iss. 1,* (May 2021). DOI:10.1088/1755-1315/664/1/012030

[23] V.N. Cococi, C.-A. Safta, C. Calinoiu, Pneumatic Actuator Controlled by Proportional Valve. Experimental results, *E3S Web of Conferences; Les Ulis, Vol. 286,* (2021). DOI:10.1051/e3sconf/202128604010

[24] V.N. Cococi, C.-A. Safta, Noi direcții de dezvoltare a sistemelor pneumatice de acționare și control, *Revista stiinta si inginerie 2018*

[25] V. N. Cococi, C. Călinoiu, C.-A. Safta, Electropneumatic Servomechanism with Proportional Direction Control Valve, *The 13th international symposium on advanced topics in electrical engineering*, March 23-25, 2023 Bucharest, Romania DOI: 10.1109/ATEE58038.2023.10108107

[26] V. N. Cococi, C. Calinoiu, Al. Marin and C. A. Safta, *Water Valves in Water Digitalization Process. Numerical and Experimental Approach, Journal of Hydroinformatics 2023* (în recenzie)

[27] V. Constantin, G. Belforte, O. Dontu, M. Avram, *U.P.B. Sci. Bull.*, Series D, Vol. 76, Iss. 4, pp 57-68, (2014).

[28] V. Cosoroaba, Th. Demetrescu, Gh. Georgescu-Azuca, *Actionari pneumatice*, Intreprinderea Poligrafica „13 Decembrie 1918" Bucuresti, pg 426-440

[29] D. M. Correia, et al. *"Networking Programmable Logic Controllers: Pneumatic Cylinder Modelling and Control." (2015).* https://www.semanticscholar.org/paper/Networking-Programmable-Logic-

Controllers%3A-Cylinder-Correia Sequeira/36c30fdf1bc97a9a87821aed23f41341d1facf9d

[30] D. E. Cristancho, L. A. Coy, K. R. Hall, G. A. Iglesias-Silva, An alternative formulation of the standard orifice equation for natural gas, Flow Measurement and Instrumentation 21 (2010) 299–301

[31] B. Cui, Zhe Lin, Zuchao Zhu, Huijie Wang, Guangfei Ma, Influence of opening and closing process of ball valve on external performance and internal flow characteristics, *Experimental Thermal and Fluid Science* 80 (2017) 193–202

[32] R. Darby, The dynamic response of pressure relief valves in vapor or gas service, part I: Mathematical model, *Journal of Loss Prevention in the Process Industries* 26 (2013) 1262e1268

[33] W. Dazhuan, Wu Peng, Li Zhifeng, Wang Leqin, The transient flow in a centrifugal pump during the discharge valve rapid opening process, *Nuclear Engineering and Design* 240 (2010) 4061–4068

[34] Z. Dimitrova, F. Maréchal, Gasoline hybrid pneumatic engine for efficient vehicle powertrain hybridization, *Ecole Polytechnique Fédérale de Lausanne*, Lausanne, Switzerland

[35] A. Djurkov, J. Cloutier, M. P. Mintchev, Mathematical model and simulation of a pneumatic apparatus for in-drilling alignment of an inertial navigation unit during horizontal well drilling, *International Journal "Information Technologies and Knowledge*" Vol.2 / 2008

[36] F. D. Dragne, M. Alirand, I. M. Oprean I M and Vasiliu N, ABS valve model reduction AMESIM, *Proc. of the Romanian Academy* A 10/2 pp189-196

[37] A. Dragomirescu, Contributții la gazodinamica ventilatoarelor de mare presiune, Teză Doctorat UPB, 2010

[38] I. M. Eross (căs. ICHIM), Rezumat teza de doctorat Cercetări teoretice şi experimentale privind creştereaperformanţelor dinamice ale acţionărilor şi comenzilor pneumatice utilizate la echipamentele logistice, Universitatea Transilvania din Braşov, Şcoala Doctorală Interdisciplinară, Centrul de cercetare: Tehnologii şi sisteme avansate de fabricaţie, BRAŞOV, 2012, pag. 13-18;

[39] A. A. M. Faudzi, K. bin Osman, M. F. Rahmat, N. D. Mustafa, M. A. Azman and K. Suzumorid, Controller Design for Simulation Control of Intelligent Pneumatic Actuators (IPA), *System Procedia Engineering* 41 593 – 599 IRIS 212

[40] K. Foit, W. Banaś and G. Ćwikła, The pneumatic and electropneumatic systems in the context of 4th industrial revolution, *IOP Conf Ser Mater Sci Eng* 400 022024 ,

[41] M. J. Fotuhi, Z. Bingul, Comparative Study of the Parallel and Angular Electrical Gripper for Industrial Applications, *Acta Mechanica et Automatica*, vol.15 no.2 (2021), DOI 10.2478/ama-2021-0010

[42] J. Gerhartz, D. Scholz, *Closed-Loop Pneumatics*, Workbook Basic Level, Festo Didactic KG, D-73734 Esslingen, 1994

[43] M. Hamdan, Z. Gao, A Novel PID Controller for Pneumatic Proportional Valves with Hysteresis, *Conference Record of the 2000 IEEE Industry Applications Conference. Thirty-Fifth IAS Annual Meeting and World Conference on Industrial Applications of Electrical Energy* (Cat. No.00CH37129)

[44] J. Hanbury, White paper. *The future role of Ethernet and the trend to decentralised control solutions*, 2015, Festo AG & Co.

[45] S. Hodgson, M. Q. Le, M. Tavakoli, M. T. Pham, Sliding-Mode Control of Nonlinear Discrete-Input Pneumatic Actuators, *IROS*, San Francisco, CA : United States (2011)", DOI : 10.1109/IROS.2011.6048194

[46] K. D. Huang, H.-N.Nguyen, Aspect of Dynamic Simulation and Experimental Research Studies on Hybrid Pneumatic Power System, *Hindawi Publishing Corporation International Journal of Vehicular Technology Volume* 2010, Article ID 893197, 13 pages doi:10.1155/2010/893197

[47] A. Ilchmann, Oliver Sawodny, Stephan Trenn, Pneumatic cylinders: modelling and feedback force-control, *Institut fur Mathematik, Technische Universitat Ilmenau, Weimarer Straße* 25, 98693 Ilmenau, DE;achim.ilchmann@tu-ilmenau.de, stephan.trenn@tu-ilmenau.de, 2 May 20

[48] N. Ion, V. N. Cococi, C. Călinoiu and C.-A. Safta, Controlling the air flow rate in a wastewater treatment plant bioreactor by using pneumatic proportional valves*, 11th International Conference on ENERGY and ENVIRONMENT (CIEM)* (recenzat, în curs de aparitie)

[49] A. Irawan, M. S. Ramli, M. H. Sulaiman, M. I. P. Azahar, A. H. Adom, Optimal Pneumatic Actuator Positioning and Dynamic Stability using Prescribed Performance Control with Particle Swarm Optimization: A Simulation Study, *International Journal of Robotics and Control Systems*, Vol. 3, No. 3, 2023, pp. 364-379

[50] A. K. Jaliel and M. F. Badr, Application of Directional Control Solenoid Valves in Pneumatic Position System, 2020 *IOP Conf. Ser.: Mater. Sci. Eng*. 870 012044

[51] K. N. Kamaludin, L. Abdullah, S. N. S. Salim, Z. Jamaludin, N. A. Rafan, M. F. Rahmat and R. Ramanathan, Triple nonlinear hyperbolic pid with static friction compensation for precise positioning of a servo pneumatic actuator, *IIUM Engineering J.*, Vol. 24, No. 2, 2023 https://doi.org/10.31436/iiumej.v24i2.2766

[52] M. Karpenko and N. Sepehri, "Design and experimental evaluation of a nonlinear position controller for a pneumatic actuator with friction," in *Proceedings of the 2004 American Control Conference*, vol. 6, pp. 5078-5083, 2004, https://doi.org/10.23919/ACC.2004.1384656

[53] J. Ke, J. Wang, N. Jia, L. Yang, Q. H. Wu, Energy Efficiency Analysis and Optimal Control of Servo Pneumatic Cylinders, Proceedings of the 2005 *IEEE Conference on Control Application*s, Toronto, Canada, August 28-31, 2005

[54] Ir. C. Kleijn, Modeling and simulation of fluid power systems using 20-sim, *Controllab Products B.V Hengelosestraat* 705, 7521 PA, Enschede, The Netherlands, https://www.20sim.com/downloads/Factsheets/Factsheet%20Fluid.pdf

[55] W. Kobayashi, N. Kato, S. Dohta, T. Akagi, Position Control of Flexible Pneumatic Cylinder Using Tiny Embedded Controller with Disturbance Observer, *Int. J. of Mechanical Engineering and Robotics Research* Vol. 6, No. 4, 318-321 (2017)

[56] I. Krivits, G. V. Krejnin, *Pneumatic Actuating Systems for automatic equipment. Structure and design*, (CRC Press Press Taylor and Francis Group 2006).

[57] G. Kritikov, M. Strizhak, V. Strizhak, Concept, circuit diagram and algorithm for controlling multi-position pneumatic actuator with adaptive positioning mode, *U.P.B. Sci. Bull.*, Series D, Vol. 83, Iss. 1, 2021 ISSN 1454-2358

[58] V. Kumar and A. P. Mittal, Dynamic Modeling of Liquid-Flow Process due to Hysteresis of Pneumatic Control Valve, *International Journal of intelligent control and systems* vol.15,NO.1,march 2010,1-8

[59] T. R. Kuphaldt – Under the terms and conditions of the Creative Commons Attribution 4.0 International Public License, *Lessons In Industrial Instrumentation*, Version 2.32 (stable) – Released 4 January 2019, pg 2341-2342

[60] A. S. Lafmejani, Mehdi Tale Masouleh, Ahmad Kalhor, An Experimental Study on Friction Identification of a Pneumatic Actuator and Dynamic Modeling of a Proportional Valve, *Proceedings of the 4th International Conference on Robotics and Mechatronics*, October 26-28, 2016, Tehran, Iran

[61] H.-T. Lin, A Novel Real-Time Path Servo Control of a Hardware-in-the-Loop for a Large-Stroke Asymmetric Rod-Less Pneumatic System under Variable Loads, *Sensors 2017*, 17, 1283; doi:10.3390/s17061283,

[62] Z. Lin, T. Zhang, Q. Xie, Q. Wei, Electropneumatic position tracking control system based on an intelligent phase-change PWM strategy, *Journal of the Brazilian Society of Mechanical Sciences and Engineering (2018)* 40:512, https://doi.org/10.1007/s40430-018-1431-y

[63] Ł. Magdziak, I. Malujda, D. Wilczyński, D. Wojtkowiak, 2017, Concept of improving positioning of pneumatic drive as drive of manipulator, *Procedia Engineering* 177 331 – 338

[64] N. Manafi, *Curs Mecanica Aplicata*, Partea a III a, Autor, pag 156, link: https://cursmecanica.blogspot.com/2011/01/bazele-mecanicii-aplicate.html

[65] A. Mehmood, S. Laghrouche, M. El Bagdouri, Control of the Electropneumatic VGT Actuator with Friction Compensators, *18th World Congress The International Federation of Automatic Control Milano* (Italy) August 28 - September 2, 2011

[66] J. Mei, S. Xie, H. Liu, J. Zang, Hysteresis Modelling and Compensation of Pneumatic Artificial Muscles using the Generalized Prandtl-Ishlinskii Model, Strojniški vestnik - *Journal of Mechanical Engineering* 63(2017)11, 657-665, DOI:10.5545/sv-jme.2017.4491

[67] G. Mikulowski and R. Wiszowaty, *Research Article* Pneumatic Adaptive Absorber: Mathematical Modelling with Experimental Verification, Hindawi Pub. Co., Mathematical Problems in Engineering, Volume 2016, Article ID 7074206, 13 pages, http://dx.doi.org/10.1155/2016/7074206

[68] F. Mohamed, A. A. Dahoud, Integrated Development Environment "IDE" For Arduino(2018)https://www.researchgate.net/publication/328615543_Integrated_Development_Environment_IDE_For_Arduino

[69] M.N. Muftah, A.A.M. Faudzi, S. Sahlan, and S. Mohamaddan, Fuzzy Fractional Order PID Tuned via PSO for a Pneumatic Actuator with Ball Beam (PABB) System. *Fractal Fract.* 2023, *7*, 416. https://doi.org/10.3390/ fractalfract7060416

[70] G. A. Muzy, A. S. Caporali, Positioning system of a pneumatic actuator driven by proportional pressure regulator valves, *Proceedings of the 4th Workshop on Innovative Engineering For Fluid Power* – WIEFP 2018, 28-30 November 2018, ABIMAQ, São Paulo, SP, Brazil, DOI: 10.3384/ecp1815611.

[71] M. Avram, C. Bucșan, *Sisteme de acționare pneumatice inteligente*, Ed. Politehnica Press, 2014

[72] B. Najjari, S. M. Barakati, A. Mohammadi, M. J. Fotuhi, S. Farahat, and M. Bostanian, Modelling and Controller Design of Electropneumatic Actuator Based on PWM, *International Journal of Robotics and Automation (IJRA)*, Vol. 1, No. 3, September 2012, pp. 125~136

[73] B. Najjari, S. M. Barakati, A. Mohammadi, M. J. Futohi, M. Bostanian, Position control of an electropneumatic system based on PWM technique and FLC, *ISA Transactions* 53 (2014) 647–657

[74] F. Ning, Y. Shi, M. Cai, Y. Wang and W. Xu, Research Progress of Related Technologies of Electric-Pneumatic Pressure Proportional Valves, *Appl. Sci.* **2017**, *7*, 1074; doi:10.3390/app7101074

[75] S. Ning, and G. M. Bone, Development of a Nonlinear Dynamic Model for a Servo Pneumatic Positioning System, *Proceedings of the IEEE International Conference on Mechatronics and Automation*, Niagara Falls, Canada, pp.43-48, 2005. DOI: 10.1109/ICMA.2005.1626520

[76] S. Ning, and G. M. Bone, High Steady-State Accuracy Pneumatic Servo Positioning System with PVA/PV Control and Friction Compensation, *Proceedings of the 2002 IEEE International Conference on Robotics and Automation, Washington*, DC, pp. 2824-2829, 2002. DOI: 10.1109/ROBOT.2002.1013660

[77] B. M. Y. Nouri, Ma'ali B. Y. Saudi, Experimental Modelling and Identification of Compressible Flow through Proportional Directional Control Valves, *Universal Journal of Control and Automation* 2(1): 4-13, 2014, DOI: 10.13189/ujca.2014.020102

[78] K. Osman, A. 'A. M. Faudzi, M. F. Rahmat, and K. Suzumori System Identification and Embedded Controller Design for Pneumatic Actuator with Stiffness Characteristic, *Hindawi Publishing Corporation Mathematical Problems in Engineering Volume 2014*, Article ID 271741, 13 pages http://dx.doi.org/10.1155/2014/271741

[79] R. Piotrowski, H. Sawicki, and K. Żuk, "Novel hierarchical nonlinear control algorithm to improve dissolved oxygen control in biological WWTP," *Journal of Process Control* 105 (2021) 78–87, https://doi.org/10.1016/j.jprocont.2021.07.00

[80] H. Qi, Gary M. Bone, Yile Zhang, Position Control of Pneumatic Actuators Using Three-Mode Discrete-Valued Model Predictive Control, https://doi.org/10.3390/act8030056

[81] M. G. Rabie, *Fluid Power Engineering*, (Ed. McGraw Hill Companies, 2009).

[82] Vs. Radcenco, N. Alexandrescu, E. Ionescu, M. Ionescu, *Calculul și proiectarea elementelor și schemelor pneumatice de automatizare*, Ed Tehnică, București, 1985

[83] M.F. Rahmat, S. N. S. Salim, A. 'Athif Mohd Faudzi, Z. H. Ismail, S. I. Samsudin, N. H. Sunar, K. Jusoff, Non-linear Modeling and Cascade Control of an Industrial Pneumatic Actuator System, *Australian Journal of Basic and Applied Sciences*, 5(8): 465-477, 2011, ISSN 1991-8178

[84] M. F. Rahmat, N. H Sunar and Sy Najib Sy Salim, Mastura Shafinaz Zainal Abidin , A. A Mohd Fauzi and Z. H. Ismail, Review on Modeling and Controller Design in Pneumatic Actuator Control System, *International Journal on smart sensing and intelligent systems* vol. 4, no. 4, december 2011

[85] M. F. Rahmat, Sy Najib Sy Salim, N. H. Sunar, Ahmad 'Athif Mohd Faudzi, Zool Hilmi Ismail and K. Huda, Identification and non-linear control strategy for

industrial pneumatic actuator, *International Journal of the Physical Sciences* Vol. 7(17), pp. 2565 - 2579, 23 April, 2012, DOI: 10.5897/IJPS12.030

[86] I. Ramírez*,* Modeling and tracking control of a pneumatic servo positioning system. *2013 II International Congress of Engineering Mechatronics and Automation (CIIMA) (2013): 1-6.*

[87] I. Ramírez, *Design of a tracking controller of a siso system of pneumatic servopositioning*, Ingeniería y Desarrollo, vol. 36, no. 1, 2018, January-June, pp. 74-96

[88] Z. Rao, and G. M. Bone, Nonlinear Modeling and Control of Servo Pneumatic Actuators, *IEEE Transactions on Control Systems Technology*, Vol. 16, pp. 562-569, 2008. DOI: 10.1109/TCST.2007.912127

[89] E. Richer, Y. Hurmuzlu, A High Performance Pneumatic Force Actuator System. Part 1 - Nonlinear Mathematical Model, ASME *Journal of Dynamic Systems Measurement and Control*, Vol. 122, No.3, pp. 416-425, (2001).

[90] C. S. Ritter, Valdiero A. C., Andrighetto P. L., Zago F., Endler L., Nonlinear characteristics Systematic Study in Pneumatic Actuators, *ABCM Symposium series in Mechatronics*, Vol. 4, pp 818-826, 2010.

[91] J. Rwafa, F. Ghayoor, Implementation of Iterative Learning Control on a Pneumatic Actuator. *Actuators* **2022**, *11*, 240. https://doi.org/10.3390/act11080240

[92] C. A. Safta, V. N. Cococi, C. Călinoiu and Al. Marin, Performance of water valves required by water supply network digitalization process, *14th International Conference on Hydroinformatics HIC 2022 − Water INFLUENCE, IOP Conference Series. Earth and Environmental Science; Bristol Vol. 1136, Iss. 1, (Jan 2023)*: 012051. DOI:10.1088/1755-1315/1136/1/012051

[93] B. K. Saha, H. Chattopadhyay, P. B. Mandal, Tapas Gangopadhyay, Dynamic simulation of a pressure regulating and shut-off valve, *Computers & Fluids* 101 (2014) 233–240

[94] S. N. S. Salim, A. A. M. Faudzi, Z. H. Ismail, M.F. Rahmat, N.H.Sunar, S. A. Samsudin, Practical robust control using Self-regulation Nonlinear PID controller for pneumatic positioning system, *Proceeding of International Conference on Electrical Engineering, Computer Science and Informatics (EECSI 2014)*, Yogyakarta, Indonesia, 20-21 August 2014

[95] S. N. S. Salim, M. F. Rahmat, A. 'A. M. Faudzi, Z. H. Ismail, and N. Sunar, Position Control of Pneumatic Actuator Using Self-Regulation Nonlinear PID, *Hindawi Publishing Corporation Mathematical Problems in Engineering Volume 2014*, Article ID 957041, 12 pages http://dx.doi.org/10.1155/2014/957041

[96] S. I. Samsudin, S. F. Sulaiman, K. Osman, S. I. M. Salim, S. N. M. Azam, Development of Nonlinear Adaptive PI Controller ForImproved Pneumatic Actuator System, *Int. J. of integrated engineering vol*. 14 NO. 6 (2022) 206 - 215

[97] D. Saravanakumar, B. Mohan, T. Muthuramalingam, A review on recent research trends in servo pneumatic positioning systems, *Precision Engineering* 49 (2017) 481–492

[98] J.L. Shearer, Study of Pneumatic Process in the Continuous Control of Motion with Compressed Air, *Trans. ASME 1956*, 2, pp 233–242.

[99] M. Sorli, L. Gastaldi, E. Codina, S. de las Heras, Dynamic analysis of pneumatic actuators, Simulation Practice and Theory 7 (1999) 589–602

[100] M. Sorli, L. Gastaldi, Thermic Influence on the Dynamics of Pneumatic Servosystems, *J. of Dynamic Systems Measurement and Control* 01/2009; 131(2). DOI:10.1115/1.3072115

[101] M. Stankovic, A. Hasanbeigi and N. Neftenov, 2020 *Use of 4IR Technologies in Water and Sanitation in Latin America and the Caribbean* (technical report), Inter-American Development Bank

[102] A. M. Stănescu, V. Gh Banu, M. Atodiroaei, V. Găburici, *Sisteme de automatizare pneumatice. Proiectarea asistată de calculator a blocurilor funcționale*, Ed. Tehnică, 1987.

[103] Y. Tassa, T. Wu, J. Movellan∗ & E. Todorov, *Modeling and Identification of Pneumatic Actuators*, 2013, DOI: 10.1109/ICMA.2013.6617958

[104] A. C. Valdiero, C. S. Ritter, C. F. Rios and M. Rafikov, Non Linear Mathematical Modeling in Pneumatic Servo Position Applications, *Hindawi Publishing Corporation Mathematical Problems in Engineering* Article ID 472903 doi:10.1155/2011/47290

[105] N. Vasiliu, D. Vasiliu, C. Călinoiu, R. Puhalschi, *Simulation of fluid power systems with Simcenter Amesim*, (Ed. CRC Press Taylor and Francis Group 2018).

[106] J. Wang, J. Pu, and P. R. Moore, A practicable control strategy for servo pneumatic actuator systems. *Control Eng. Pract.*, 1999, **7**, 1483–1488.

[107] J. Wang, D. J. D. Wang, P. R. Moore, and J. Pu, Modeling study, analysis and robust servo control of pneumatic cylinder actuator systems. *IEE Proc. Control Theory Appl.*, 2001, 148, 35–42.

[108] J. Wang, U. Kotta, and J. Ke, Tracking control of nonlinear pneumatic actuator systems using static state feedback linearisation of input/output map, *Proc. Estonian Acad. Sci. Phys. Math.*, vol. 56, pp. 47–66, 2007.

[109] G. Yang, P. Jiang, L. Lei, Y. Wu, J. Du, and B. Li, Adaptive Backstepping Control of Vacuum Servo System Using High-Speed on-off Valves, *IEEE Access*, Vol. 8, 2020, DOI 10.1109/ACCESS.2020.3007208

[110] Y. Yin, High Speed Pneumatic Theory and Technology Volume I. *Servo System, ed. Springer*, 2019, https://doi.org/10.1007/978-981-13-5986-6

[111] L. Zhao, Y. Xia, H. Yang, J. Zhang, Pneumatic Servo Systems Analysis. Control and Application in Robotic Systems, *Ed. Springers*, 2022, ISSN 2193-1577

[112] R. Zhihong, and B. Gary, 2008. Nonlinear modeling and control of servo pneumatic actuators, *IEEE, Transactions on Control Systems Technology*, 16(3): 562-569.

[113] ***https://www.tomorrowsworldtoday.com/2021/07/26/history-of-pneumatics/

[114] *** MEC-E5003 Fluid Power Basics, Brief history of pneumatics

[115] ***https://www.grandviewresearch.com/industry-analysis/pneumatic-conveying-system-market

[116] ***https://www.databridgemarketresearch.com/reports/global-pneumatic-components-and-systems-market

[117] ***https://library.automationdirect.com/why-use-pneumatics

[118] ***https://nptel.ac.in/courses/112106175/Module%204/Lecture%2033.pdf

[119] ***https://airo-pneumatics.ro/2015/09/17/capitolul-5-distribuitoare-pneumatice-introducere/

[120] ***http://www.flupec.ro/produse/pneumatica/accesorii-pneumatice/supape/supape-de-sens-pneumatice/supapa-de-sens-6063

[121] ***http://www.rasfoiesc.com/inginerie/electronica/SUPAPE-DE-PRESIUNE31.php

[122] ***https://www.primabt.ro/produse/detalii-produs/drosere-aer-comprimat/

[123] ***http://www.asconumatics.eu/tr/urunler/kataloglar/pneumatic-components-for-industrial-automation/pneumatic-proportional-valves.html

[124] ***https://www.festo.com/cat/ro_ro/products_010000

[125] ***https://airo-pneumatics.ro/2015/08/27/capitolul-4-motoare-pneumatice-oscilante/

[126] ***https://www.operatorserv.ro/produse/actionari-pneumatice-rotative.html

[127] ***https://www.festo.com/rep/be_by/assets/pdf/Druckluftaufbereitung_en.pdf

[128] ***http://www.nptel.ac.in/courses/112102011/electropenumatics/relay%20control%20system.html

[129] ***https://reactivesystems.wordpress.com/2012/02/11/pneumatic-actuators/

[130] ***https://inductiveautomation.com/what-is-iiot

[131] ***https://www.controldesign.com/articles/2016/ethernet-vs-fieldbus-the-right-

[132] ***https://www.scribd.com/doc/57467901/Miscarea-Rectilinie-Uniforma

[133] *** https://www.festo.com/cms/ro_ro/64621.htm

[134] ***https://www.schneider-servohydraulics.com/en/products/pneumatic-servo-valves/

[135] ***https://www.smcworld.com/webcatalog/en-jp/modular-frl-units-pressure-control-equipment/proportional-valves/

[136] ***Simulink® Getting Started Guide, https://www.mathworks.com/help/simulink/, deschis in 13.05.2020, ora 14:30

[137] ***https://www.plm.automation.siemens.com/global/en/products/simcenter/simcenter-amesim.html, deschis in 13.05.2020, ora 14:50

[138] ***https://en.wikipedia.org/wiki/VisSim, deschis in 13.05.2020, ora 15:20

[139] ***https://en.wikipedia.org/wiki/Dymola, deschis in 13.05.2020, ora 15:40

[140] ***https://www.mscsoftware.com/product/easy5 , deschis in 15.05.2020, ora 08:40

[141] ***https://www.festo-didactic.com/ro-ro/sisteme-de-inv-tare/factory-automation-industry-4.0/industrial-control-technology/588/universal-connection-unit,digital-syslink.htm?fbid=cm8ucm8uNTcwLjM1LjE4LjU4OC4zNjAw

[142] ***https://www.festo-didactic.com/ro-ro/sisteme-de-inv-tare/digital-learning/fluidsim/easyport-usb-an-interface-for-measuring,open-loop-control,closed-loop-control.-connects-the-simulation-to-the-real-world.htm?fbid=cm8ucm8uNTcwLjM1LjE4LjU5MS41Mzgy

[143] ***andaccessories.htm?fbid=cm8ucm8uNTcwLjM1LjE4LjU2NC4zOTAx (site accesat in data de 01.06.2021 ora 21:20)

[144] ***https://www.festo-didactic.com/ro-ro/sisteme-de-inv-tare/fluid-power/562/components/linear-potentiometer-position-encoder.htm?fbid=cm8ucm8uNTcwLjM1LjE4LjU2NC4zNDcx (site accesat in data de 01.06.2021 ora 21:20)

[145] ***https://www.festo-didactic.com/ro-ro/sisteme-de-inv-tare/fluid-power/502/components/pid-controller.htm?fbid=cm8ucm8uNTcwLjM1LjE4LjU2MC4zNjE2 (site accesat in data de 01.06.2021 ora 21:23)

[146] ***https://www.festo-didactic.com/ro-ro/sisteme-de-inv-tare/fluid-power/562/components/5-3-way-proportional-valve.htm?fbid=cm8ucm8uNTcwLjM1LjE4LjU2NC4zNjcz (site accesat in data de 01.06.2021 ora 21:23)